

AD621521

AD

# USAALABS TECHNICAL REPORT 65-53

## THEORETICAL ANALYSIS OF AIRCRAFT ELECTROSTATIC DISCHARGE

### FINAL REPORT

By

DDC

Juan de la Cierva  
Herbert J. Gillis  
Paul B. Wilson, Jr.

OCT 6 1965

JIA B

August 1965

U. S. ARMY AVIATION MATERIEL LABORATORIES  
FORT EUSTIS, VIRGINIA

CONTRACT DA 44-177-AMC-82(T)

DYNASCiences CORPORATION



CLEARINGHOUSE FOR FEDERAL SCIENTIFIC AND TECHNICAL INFORMATION	
Hardcopy	Microfiche
\$4.00	0.75
120 pp	ea
ARMED FORCES COPY	

DDC Availability Notices

Qualified requesters may obtain copies of this report from DDC.

This report has been furnished to the Department of Commerce for sale to the public.

Disclaimers

The findings in this report are not to be construed as an official Department of the Army position, unless so designated by other authorized documents.

When Government drawings, specifications, or other data are used for any purpose other than in connection with a definitely related Government procurement operation, the United States Government thereby incurs no responsibility nor any obligation whatsoever; and the fact that the Government may have formulated, furnished, or in any way supplied the said drawings, specifications, or other data is not to be regarded by implication or otherwise as in any manner licensing the holder or any other person or corporation, or conveying any rights or permission, to manufacture, use, or sell any patented invention that may in any way be related thereto.

Disposition Instructions

Destroy this report when it is no longer needed. Do not return it to the originator.



DEPARTMENT OF THE ARMY  
U S ARMY AVIATION MATERIEL LABORATORIES  
FORT EUSTIS, VIRGINIA 23604

The research and theoretical analysis reported herein was sponsored by the U.S. Army Aviation Materiel Laboratories, Fort Eustis, Virginia, in an effort to understand more clearly the physical phenomena and processes which take place in the corona discharge process and its application to an electrostatic discharger for helicopters. As a primary part of this effort, appropriate theory was to be developed which would allow the design of helicopter electrostatic dischargers on a scientific rather than empirical basis.

This command concurs in the recommendations and conclusions made herein. As funds become available for additional research in this area, it is anticipated that other, more sophisticated, means of prevention of electrostatic buildup will be investigated.

Task 1P121401A14130  
Contract DA 44-177-AMC-82(1)  
USAAVLABS Technical Report 65-53  
August 1965

THEORETICAL ANALYSIS OF  
AIRCRAFT ELECTROSTATIC DISCHARGE

FINAL REPORT

Dynasciences Report No. DCR-132

by

Juan de la Cierva  
Herbert J. Gillis  
Paul B. Wilson, Jr.

Prepared by

Dynasciences Corporation  
Blue Bell, Pennsylvania

for

U. S. Army Aviation Materiel Laboratories  
Fort Eustis, Virginia

## SUMMARY

The general problem of aircraft electrostatic charging and one of the more efficient discharger systems presently available are discussed. Methods of discharger system design and analysis are developed and stated for this system. These methods are incorporated into design curves and other data to facilitate and optimize design.

The problem of efficient discharge corona electrode design is treated extensively. With the information on corona developed in the report, it becomes possible to include the corona electrode in the system design using conventional engineering design methods. Data permitting optimization of corona electrode performance, that is, current maximization at a given electrode voltage is given. The effects of aircraft altitude are significant on electrode operation.

Numerous approaches to the reduction of system voltage requirements are discussed.

## FOREWORD

The Dynasciences Corporation, under the sponsorship of the U.S. Army Aviation Materiel Laboratories\* (USAAML), Fort Eustis, Virginia, has conducted a study to provide the theory for the efficient design and optimization of aircraft electrostatic discharging systems. The investigators were Messrs. Juan de la Cierva, Herbert J. Gillis, and Paul B. Wilson, Jr. The cognizant USAAVLABS project officer was Mr. S. Blair Poteate, Jr.

The project was conducted during the period June 1963 through January 1964.

The continuing interest of the U.S. Army Aviation Materiel Laboratories in helicopter performance improvement made possible this contribution to aircraft electrostatic discharging and is gratefully acknowledged.

---

\*Formerly, U.S. Army Transportation Research Command.

## CONTENTS

	<u>Page</u>
SUMMARY	iii
FOREWORD	v
LIST OF ILLUSTRATIONS	viii
LIST OF SYMBOLS	x
SECTION A: INTRODUCTION	1
SECTION B: CORONA POINT-AIRCRAFT FUSELAGE CONFIGURATION	4
SECTION C: CORONA DISCHARGE IN STILL AIR	11
SECTION D: CALCULATION OF CORONA CURRENT IN MOVING AIR	33
SECTION E: EFFECTS OF ATMOSPHERIC CONDITIONS	62
SECTION F: INVESTIGATION OF CORONA PROBE PERFORMANCE IMPROVEMENT	65
SECTION G: DISCHARGER SYSTEM OPERATION AND ANALYSIS	69
CONCLUSIONS	91
RECOMMENDATIONS	91
BIBLIOGRAPHY	92
DISTRIBUTION	95
APPENDIXES	
I. Derivation of Equations for Design Curves	97
II. Analog Computer Analysis of Discharger System Dynamics	99

## ILLUSTRATIONS

<u>Figure</u>		<u>Page</u>
1	Typical Corona Probe Configurations for Single and Tandem Rotor Helicopters	5
2	Determination of the Electrostatic Field in a Point-Plane Geometry	8
3	Minimum Negative Probe Voltage Required for Initiating Corona as a Function of Electrode Tip Radius and Spacing From Aircraft	19
4	Minimum Positive Probe Voltage Required for Initiating Corona as a Function of Electrode Tip Radius and Spacing From Aircraft	29
5	Corona Discharge Current in Still Air	31
6	Force Vectors Acting on a Charged Particle at $h = c$	40
7	Force Vectors Acting on a Charged Particle at $h = c/2$	41
8	Particle Balance Diagram for Infinitesimal Volume	54
9	Corona Discharge Current Versus Electrode Voltage for Two Wind Speeds in a Typical Discharger System	61
10	Effect of Pressure Change Due to Altitude on Corona Electrode Performance	63
11	Corona Current Discharge for Various Corona Point Configurations	69

<u>Figure</u>		<u>Page</u>
12	Block Diagram, Aircraft Static Electricity Discharging System	72
13	Electrostatic Discharger System Diagram	74
14	Typical Mounting of Corona Discharge Electrode on a Tandem Rotor Helicopter	76
15	Design Curves for Electrostatic Discharger	82
16	Operation of Passive Corona Point Sensor	87
17	Dynamic Discharger System Diagram	87
18	CVSS Electrostatic Discharger Functional Block Diagram	98
19	Analog Computer Diagram	101

A	current emissive surface area of corona electrode
C	constant appearing in corona current equation depending on radius of corona point and point-plane separation
$C_C$	compensator capacitance
$C_D$	coefficient of aerodynamic drag
$C_H$	aircraft capacitance at a specific altitude
$C_{HM}$	maximum aircraft capacitance
c	distance from corona point to virtual anode, that is, to finite conducting plane Figure 2
$D_i$	diffusion coefficient for charged particles
d	diameter of sphere approximating ion
E	electrical field intensity
$E_A$	electrostatic stored energy of aircraft
$E_B$	field strength vector at point B
$E_D$	field strength at discharger electrode
$E_H$	electrostatic field of aircraft surface at sensor location
$E_i$	electrostatic field strength for charged particles
$E_T$	actual electrostatic field strength
$E_{u.v.}$	ultraviolet photon energy
$E_w$	equivalent electric field strength representing viscous effects on ions
e	napierian base

$e$	electrical charge of an electron
$F$	force
$F_{c,1}$	closed loop gain of GVSS Dynasciences Corporation electrostatic discharger system; ratio of output $I_d$ to input $I_t$
$\hat{F}_e$	electric force vector on the charged particle
$F_r$	pulse repetition rate of Trichel pulses of corona current
$F_{o,1}$	open loop gain of GVSS Dynasciences Corporation electrostatic discharger system; ratio of output $I_d$ to input $I_t$
$\hat{F}_t$	vector total force on the charged particles at any instant
$\hat{F}_w$	vector viscous wind force at any instant
$f$	denotes function of
$f$	frequency of ultraviolet light
$f_p$	proportionality constant relating the number of electrons in a Townsend avalanche to the number of photons they produce, Reference 19
$h$	distance from infinite conducting plane to corona tip Figure 2
$h_p$	planck constant
$I$	average corona current
$I_d$	corona discharge current
$I_n$	time rate of charge acquisition by the aircraft due to natural atmospheric conditions

$I_t$	net current charging the aircraft-the difference between $I_n$ and $I_d$
$i$	instantaneous corona current
$i_o$	current charge per second at corona electrode surface
$J_i$	current density of charged particles
$J_t$	total current per unit area equalling the sum of the electron and positive ion current per unit area, a constant in the steady state
$K$	overall steady state gain of discharger system-the ratio of steady state system output $V_H$ to the system input $I_n$
$K_a$	transfer function of power amplifier relating output $V_a$ and $V_c$
$K_{cl}$	multiplying factor of transfer function of the control unit of GVSS electrostatic discharger system.
$K_{cp}$	transfer function of corona point relating output corona current to input corona point voltage
$K_g$	steady state gain of high voltage generator
$K_x$	amplitude of step input
$K_{neg}$	transfer function of negative corona point in dynamic neutralizer discharger system
$K_{pos}$	transfer function of positive corona point in dynamic neutralizer discharger system
$K_{SEN}$	transfer function of sensor
$k_B$	Boltzmann's gas constant

$k_i$	mobility of charged particles
$k_r$	constant of proportionality between $F_r$ and $v$
$m$	number of ions involved in one current pulse
$m_i$	ion mass
$N$	number of molecules per unit volume
$n_i$	number of charged particles entering unit volume per second
$n_o$	number of electrons emitted at the negative corona electrode
$n_{oA}$	number of ions emitted at corona electrode per unit area
$n_{ol}$	number of electrons emitted at corona point due to cosmic, artificial, or photo irradiation in the absence of secondary emission
$n_{o2}$	number of electrons emitted at corona point due to cosmic, artificial, or photo irradiation except the effects of secondary emission are included
$\vec{n}_1$	unit vector, direction defined in Figure 2
$\vec{n}_2$	unit vector, direction defined in Figure 2
$P_i$	normal component of electric displacement vector for charged particles
$p$	atmospheric pressure in units of mm Hg
$Q_H$	charge on aircraft
$q$	charge on sphere
$q_i$	rate of ambient ion generation due to natural or artificial causes in units of ions per unit volume per second

$q_0$	charge on probe tip
$q_r$	dynamic pressure
R	distance perpendicular to corona probe as in Figure 2
$R_e$	reynolds number
$R_s$	radius of isolated charged sphere approximating aircraft
$R_t$	radius of curvature of corona electrode or point
$R1, R2$	resistance values used in Figure 15
r	fraction of atoms ionized in each mole of engine exhaust
S	projected area of ion, assumed spherical
$S_a$	surface area of infinitesimal element
$S_\alpha$	specific ionization for alpha particles
s	laplace operator
T	absolute temperature
t	time in seconds
$t_c$	time constant of corona point high voltage supply effectively replacing $t_g$ through operation of the compensator unit
$t_g$	time constant of corona point high voltage supply
$V_a$	volume of infinitesimal element
$V_a$	output voltage of power amplifier-input to high voltage generator

$V_c$	potential difference at which corona discharge starts
$V_{Gneg}$	output of negative high voltage generator system in dynamic neutralizer discharger system
$V_{Gpos}$	output of positive high voltage generator system in dynamic neutralizer discharger system
$V_H$	potential the aircraft assumed caused by the net charging current $I_t$
$V_{HF}$	final aircraft potential
$V_i$	ionization potential of engine exhaust component
$V_s$	voltage output of generating voltmeter sensor
$V_1$	input voltage of compensator network, Figure 15
$V_o$	output voltage of compensator network, Figure 15
$v_i$	velocity of charged particles
$w$	wind speed
$w_c$	value of wind at which $K_{CP}$ was measured
$W_f$	work function for photoelectric emission of iron
$x$	position coordinate relative to the corona point
$\alpha$	Townsend's first ionization coefficient (Reference 19) - number of ionizing collisions per unit path length in the direction of the field
$\alpha_r$	recombination coefficient of ions in corona dis- charge
$\beta$	fraction of photons escaping absorption and which create secondary electrons by photoionization

- $\gamma$  Townsend's second ionization coefficient (Reference 19) - number of new electrons produced per positive ion due to the mechanism of ionization by positive ions, secondary emission at the negative point, and photoionization
- $\delta$  the number of collisions the electron must make before attaching to a neutral atom
- $E$  kinetic energy obtained by an ion just before collision with a molecule of the atmosphere
- $\epsilon$  permittivity of free space (MKS)
- $\lambda$  mean free path of an electron in the atmosphere
- $\lambda_1$  mean free path of an electron in the atmosphere at a pressure of 1 mm Hg
- $\nu$  kinematic viscosity
- $\rho_A$  atmospheric density
- $\rho_i$  volume charge density of charged particles
- $T$  time elapsed until an electron becomes attached to an oxygen molecule
- $\Psi$  phase angle of oscillatory transient component of system response  $V_H$  to a step input  $I_n$
- $\zeta$  system damping ratio =  $1/2 \sqrt{\frac{C_H}{K t_c}}$
- $\omega$  system natural frequency =  $\sqrt{\frac{K}{C_H t_c}}$
- $\nabla$  differential operator of vector calculus

#### SUBSCRIPTS

$i$  pertains to 1, 2, and 3 where

**1 refers to electrons**

**2 refers to positive ions**

**3 refers to negative ions**

## SECTION A: INTRODUCTION

As the role of the helicopter as an operational vehicle expands, it becomes increasingly important to deal effectively with the problem of large electrostatic charge accumulation on the aircraft. This charge is primarily caused by triboelectric effects between the rotor blades and the air through which they move. Triboelectricity has been defined as the electric charge transfer which takes place between dissimilar substances when brought into contact and subsequently separated. The charge transfer is due to the different number of atomic outer shell electrons which migrate from one substance to the other and vice versa. The interception of solid, liquid, or gaseous particles in the air by the helicopter rotor blades and fuselage produces a cumulative triboelectric interchange which results in an electrostatic charge potential and electrical energy buildup on the aircraft. The large energy transfer which can occur when the charged aircraft comes into contact with ground may present a serious hazard. The danger of electrical shock to personnel, ignition of flammable gas mixtures, and detonation of explosives severely affects cargo handling and personnel rescue operations. The hazards of electrostatic charge are eliminated if the stored electrical energy of the aircraft is kept at a level of one millijoule or less (Reference 21, page 7).

Many attempts to build aircraft electrostatic discharging systems have been made. The obvious expedient of discharging the aircraft by electrically contacting the earth or sea by cable has an associated spark hazard and introduces handling and operating problems. It is therefore an undesirable solution in many cases. Another method of preventing charge accumulation is the application of coatings to match the dielectric constant of the aircraft to that of the atmosphere (Reference 2). This method, however, has proven inadequate in preventing triboelectric charging in all operating conditions due to the fact that triboelectric charging is intrinsically a surface phenomenon, and triboelectric surface character-

istics of operational aircraft are highly dependent on surface conditions such as dust, oil, grit and other contaminant deposits, as well as snow and ice accumulations. These conditions vary in very significant amounts during the normal use, maintenance, and service of military and commercial aircraft. The use of radioactive coatings to discharge aircraft by rendering the adjacent atmosphere conductive because of ionization has also been investigated (Reference 2). It was found that an excessively large volume of atmosphere (50,000 cubic meters) had to be irradiated if the maximum health safety limit was not to be exceeded.

The use of passive corona discharger devices, such as the AN/ASA-3 wick dischargers commonly employed in fixed wing aircraft and similar devices, has been investigated and proven to be impractical for helicopters (Reference 3). The high level of aircraft potential required to discharge the relatively large charging currents frequently encountered in helicopter operations by means of these devices, results in high electrostatic energies stored on the aircraft which may exceed, by several orders of magnitude, the safe level required.

A fully successful discharger system was built by the Dynasciences Corporation under USAAML Contract DA-177-AMC-114(T). This system automatically controls the voltage difference between a corona electrode and the aircraft surface as a function of the electrostatic field existing on the aircraft's outer surface. The electrostatic field is measured by a sensitive device capable of detecting field intensities corresponding to aircraft electrostatic energies lower than the specified safe level. Therefore, the net charge on the aircraft is kept within acceptable values.

One objective of this report is to provide the appropriate theoretical analysis of dischargers of this type and of its several components in order to facilitate and improve the design of future units. Specifically, this theoretical information is intended to make possible the following improvements in the discharger:

1. Greater corona discharge current at a given voltage, that is, lower

operating voltage and, consequently,  
reduced weight and complexity.

2. Lower maintenance requirements.

3. Longer component life.

Extensive effort has been directed toward finding a method for the reduction of operating voltage in the discharger system. The increase of current dissipating capability of the corona electrode would permit this reduction. Consequently, the physics of corona and electrostatic fields are an important part of the report.

## SECTION B: CORONA POINT - AIRCRAFT FUSELAGE CONFIGURATION

Very high voltage generators are required to generate the corona discharging currents essential to maintain a low helicopter energy level under charging conditions. Recent progress in the state of the art in semiconductor high voltage rectifiers and other components permits the design and construction of highly efficient, low weight, and highly reliable high voltage D.C. generators for this purpose.

However, in addition to the generation of a high potential on a corona probe, several other parameters must be considered in order to neutralize an aircraft electrostatic charge buildup. Two such parameters are:

1. Air speed vector field in the vicinity of the corona probe.
2. Geometry of the electrostatic field generated by the probe potential.

The combination of these two factors together with the probe potential, determine the discharging capabilities of the probe.

The airspeed vector field in the vicinity of the corona probe depends on the location of the probe relative to the aircraft fuselage. To effect minimum recirculation, the airspeed vectors should point away from the fuselage as illustrated in Figure 1 for both single and tandem rotor helicopters.

For practical reasons, the corona point tip should point away from the aircraft, although the direction of the tip is not expected to significantly affect the direction of motion of the ions emitted from the probe point.

The effectiveness of multiple probes connected to the same high voltage generators was investigated during flight tests performed under Contracts DA 44-177-AMC-3(T)

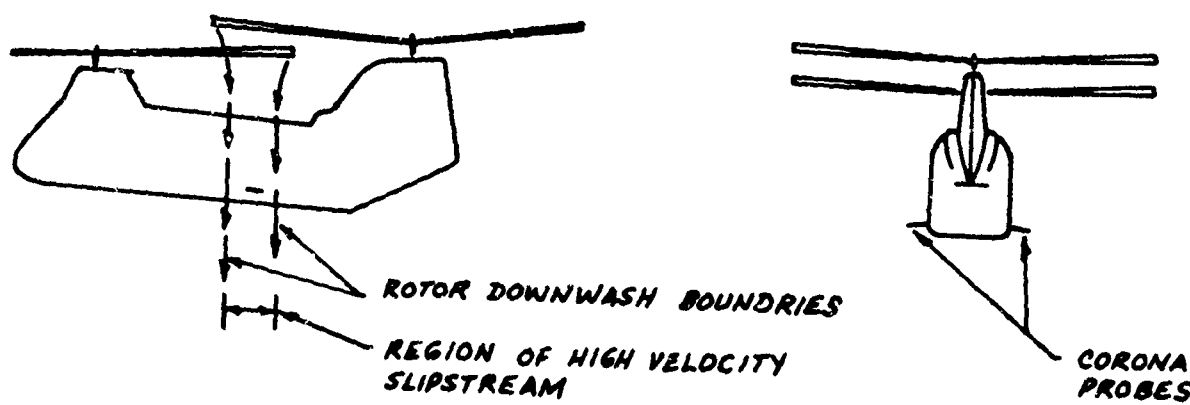
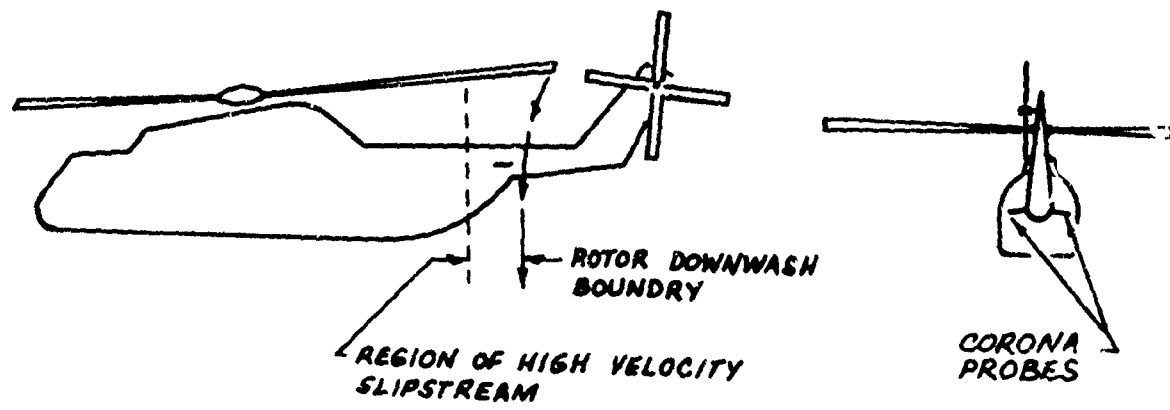


Figure 1. Typical Corona Probe Configurations for Single and Tandem Rotor Helicopters.

and DA 44-177-AMC-114(T). During the tests conducted under Contract DA 44-177-AMC-3(T), two probes which were connected to the same high voltage generators were placed on the opposite sides of the aircraft and as such were electrically shielded from each other by the aircraft structure. It was found that for the same generator voltage, the corona current of both probes was about double that of a single probe. On the other hand, under Contract DA 44-177-AMC-114(T), the two probes were mounted close together at the extremities of an externally mounted high voltage generator. The corona current for this case was found to be essentially the same as that of a single probe at the same voltage. It may be concluded, therefore, that substantial separation and shielding is required to obtain increased current by use of multiple probes. This, however, implies increased system weight and larger air drag, and considering the present state of the art, it is much more efficient to increase the voltage required to obtain the required discharge current.

The determination of the electrostatic field distribution near an active corona probe installed on an aircraft presents a classical problem of potential field theory. A generalized solution to the problem will be of little value, because the inclusion of boundary conditions closely representing aircraft fuselage configurations will make the solution to the problem extremely difficult. It is possible, however, to find a solution to the problem in some simplified geometries, such as the installation of a corona probe on an infinitely flat surface. This configuration obviously is not the one actually encountered in aircraft. However, the field distribution near the corona probe tip, will not be very different from the field distribution existent in an actual installation. The basis for this statement is the fact that near the corona tip, the main field component is due to the tip charge, the surface charge on the airframe introducing only a minor effect on the field in the tip area.

The computation of the electrostatic field of a probe placed in front of an infinitely conducting plane can be achieved by assuming a charge of equal magnitude and opposite polarity located at a point,  $P_2$ , symmetrical to the corona probe,  $P_1$ , with respect to the infinite plane. The locations of the points  $P_1$  and  $P_2$  are shown in Figure 2. The twin charge configuration renders an electrostatic field distribution in the probe side of the plane, identical to the field distribution that would result by the application between the probe and the plane of a potential of one-half that assumed between the points  $P_1$  and  $P_2$ .

To prove this similarity, let us assume there is no conductive plane between the charges at  $P_1$  and  $P_2$ . The field vector at point "0" is  $E$  and is parallel to the line between the charge points. At any other point  $B$  on the axis of symmetry the field vector  $E_B$  is parallel to the line between  $P_1$  and  $P_2$  because its two components  $E_{B1}$  and  $E_{B2}$  have the same magnitude and are symmetrical with respect to a line parallel to  $P_1 P_2$  through point  $B$ . Hence, the plane of symmetry is an equipotential surface in the field created by the charges at  $P_1$  and  $P_2$ , because the motion of a charge on it can be achieved without giving or receiving work on account of the perpendicularity between any charge path within the plane and the field vector direction on it. Thus, the resultant field on the probe side of this conductive plane will be identical to the field distribution created by the two charges at points  $P_1$  and  $P_2$ .

The field at a point  $A$ , whose coordinates are  $R$  and  $h$  can be now computed as follows.

The field due to the charge at  $P_1$  is

$$E_1 = \frac{q_0}{4\pi\epsilon_0} \left\{ \frac{P_1}{[|P_1|^2]^{3/2}} \right\} \quad (B-1)$$

but

$$P_1 = R\hat{n}_1 - (c-h)\hat{n}_2 \quad (B-2)$$

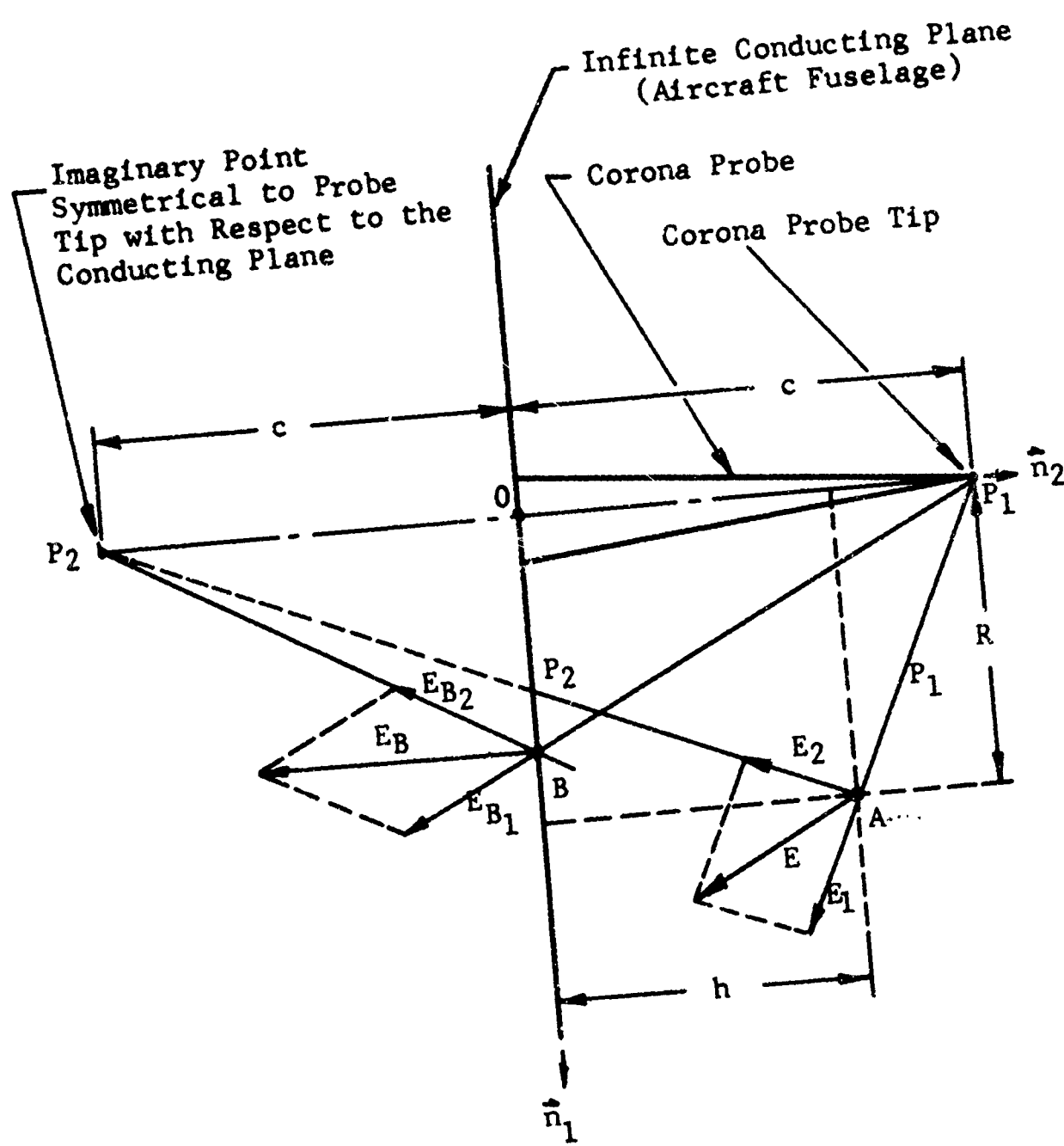


Figure 2. Determination of the Electrostatic Field  
 In a Point-Plane Geometry.

where  $\hat{n}_1$  and  $\hat{n}_2$  are two unit vectors,  $\hat{n}_1$  being perpendicular to line  $P_1P_2$  and  $\hat{n}_2$  being parallel to line  $P_1P_2$ .

The field due to the charge at  $P_2$  is

$$E_2 = \frac{q_0}{4\pi\epsilon_0} \left\{ \frac{\rho_2}{[|\rho_2|^2]^{3/2}} \right\} \quad (B-3)$$

and

$$\rho_2 = -R\hat{n}_1 - (h + c)\hat{n}_2 \quad (B-4)$$

but

$$|\rho_1|^2 = R^2 + (c - h)^2 \quad (B-5)$$

$$\text{and } |\rho_2|^2 = R^2 + (h + c)^2 \quad (B-6)$$

and the total field at A will be

$$\begin{aligned} & \frac{q_0}{4\pi\epsilon_0} \left\{ \frac{\rho_1}{[|\rho_1|^2]^{3/2}} - \frac{\rho_2}{[|\rho_2|^2]^{3/2}} \right\} \\ &= \frac{q_0}{4\pi\epsilon_0} \left\{ \frac{R}{[R^2 + (c-h)^2]^{3/2}} - \frac{R}{[R^2 + (h+c)^2]^{3/2}} \right\} \hat{n}_1 \\ & - \frac{q_0}{4\pi\epsilon_0} \left\{ \frac{c-h}{[R^2 + (c-h)^2]^{3/2}} + \frac{h+c}{[R^2 + (h+c)^2]^{3/2}} \right\} \hat{n}_2 \end{aligned} \quad (B-7)$$

The two coefficients of equation (B-7) are the magnitude of the two components of the electrostatic field parallel and normal to the conductive plane. The symmetry around the corona probe axis permits the computation of these two field vector components at any point in the space between the probe and the plane.

The field  $E$  in equation (B-7) is presented as a function of the probe charge  $q_0$ .

The relationship between the probe charge  $q_0$  and its potential with respect to the airframe can be established by using again the symmetrical charge analogy. By symmetry, it is obvious that the potential between both charges is double that of the potential between one charge and the plane of symmetry. The potential between both charges can be computed, as the work required to move a unit of charge between them against the electrostatic field of force. This potential is easily obtained for  $R = 0$ ,

$$V_p = \int_{ER=0}^{C-R_t} dh = \frac{q_0}{4\pi\epsilon_0 R_t} \left[ \frac{2(C-R_t)}{2C-R_t} \right] \quad (B-8)$$

where  $V_p$  is the potential between the charges,

$q_0$  is the charge on the probe tip, and

$R_t$  is the radius of the probe tip.

The force acting on a particle with charge  $q$  is

$$\begin{aligned} \vec{F}_e &= qE \\ &= \frac{qV_pR_t(2C-R_t)}{2(C-R_t)} \left\{ \left[ \frac{R}{[R^2 + (C-h)^2]^{3/2}} - \frac{R}{[R^2 + (C+h)^2]^{3/2}} \right] \vec{n}_1 \right. \\ &\quad \left. \left[ -\frac{c-h}{[R^2 + (C-h)^2]^{3/2}} - \frac{c+h}{[R^2 + (C+h)^2]^{3/2}} \right] \vec{n}_2 \right\} \quad (B-9) \end{aligned}$$

## SECTION C: CORONA DISCHARGE IN STILL AIR

An account of the processes occurring in corona discharge is presented as a basis for the mathematical analysis of corona given in the next section. This analysis provides a basis for the design of efficient electrostatic discharging systems. Accordingly, onset conditions, characteristics, and comparisons of positive and negative corona are given in this section. This information was derived from a study of ion generation in atmospheric corona discharge (References 6, 11, 12 and 18).

Corona is the name given to electrical conduction in a gas just before arc-over. It is distinct from other stages of conduction in that avalanche ionization takes place, and the discharge is self-sustaining, that is, no external ionization source such as cosmic radiation is necessary for its continuance. Whatever the type of gas discharge, ionization is always present since without it a gas is nonconductive. A small amount of natural ionization due to cosmic rays and radioactive trace materials suffices to trigger a discharge when a voltage is applied. An important feature of gaseous conduction is the nature of the deionization process, that is, the loss of ions constituting the discharge. This loss can occur in three ways: recombination of electrons and positive ions to neutral atoms, attachment of electrons to immobile molecules, and diffusion out of the discharge region.

### ONSET CONDITIONS AND CHARACTERISTICS OF NEGATIVE CORONA

There are three stages of discharge in the atmosphere which occur in sequence as the negative high voltage applied to the discharge electrode is increased to the corona threshold value.

#### Townsend Discharge

The values of negative voltage, being first very small, allow recombination to occur in the discharge. This causes the relationship between the discharger system electrode voltage and discharge current to be initially

linear. When the negative voltage is further increased, the ions of the discharge are drawn to the electrode before any recombination can occur. This causes current to remain constant over a small range of voltage. As voltage is still further increased, the corona discharge current begins to increase sharply. This large increase occurs because the externally caused ions, that is, ions resulting from cosmic rays or radioactive trace materials, have acquired sufficient energy to cause further ionization. The discharge, however, is not yet self-sustaining.

### Electrical Breakdown

The initial phase of breakdown is ionization by the process of externally caused ionization. This condition is termed "electron avalanche". The positive ions resulting from the avalanche generate new electrons by ionizing air molecules while being drawn to the negative electrode. Also, electrons are generated by secondary emission when these positive ions strike the negative electrode. A condition is reached as voltage is increased in which, on the average, the products of one avalanche produce at least one electron capable of starting a second avalanche as large as the first. An equilibrium between ionization and deionization follows and the discharge, being independent of external sources of ionization, becomes self-maintaining. This condition is termed "electrical breakdown" and is present in corona discharge

The ability of an electron to cause ionization and subsequent breakdown, and therefore contribute to the discharge current, depends on the energy it receives from the electric field between collisions with the air molecules. This energy is given by

$$\mathcal{E} = E \lambda e \quad (C-1)$$

where  $E$  = electric field strength,

$\lambda$  = average distance the electron travels between collisions,

$\mathcal{E}$  = ion kinetic energy increase, and

$e$  = electrical charge of an electron.

The quantity  $\lambda$  is directly proportional to temperature and is inversely proportional to pressure. Hence, at constant temperature

$$\mathcal{E} = \lambda, \frac{Ee}{p} \quad (C-2)$$

where  $\lambda$ , = mean free path of an electron at 1 mm Hg and

$p$  = atmospheric pressure in units of mm Hg.

Therefore, the electrical quantity of importance in corona discharge current calculations at constant temperature is  $E/p$ .

The expression for discharge current density provides the mathematical condition for corona onset. This expression can be calculated by the use of Townsend's first and second ionization coefficients (Reference 19). They are, respectively,

$\alpha$  = number of ionizing collisions per unit length of path in the direction of the field, and

$\gamma$  = number of new electrons produced per positive ion due to any or all of the mechanisms of ionization by positive ions, secondary emission at the negative point, and photo-ionization.

The quantity  $\alpha$  depends on the energy of the colliding electron, that is  $E/p$ , and the number of collisions per unit path length which is directly proportional to pressure, that is,

$$\alpha = \rho f(E/p) \quad (C-3)$$

Therefore,  $\alpha/p$  depends on  $E/p$  only. The second ionization coefficient  $\gamma$  depends on the material of the point and the gas. It takes into account the emission of secondary electrons by the positive ions which is not significant until the latter stages of breakdown.

Before calculating current density, the electrode geometry must be specified. The discharger system electrode geometry is most closely simulated by a point conductor (corresponding to the corona electrode) suspended over an infinite plane (corresponding to the aircraft) at a specified distance. To a close approximation, the field varies only with the position between point and plane. The distance from the point conductor along the perpendicular to the infinite plane from the point is the X coordinate.

Let the rate of natural or artificial ionization triggering the breakdown be distributed uniformly in the inter-electrode space with a magnitude of  $q_i$  ions per unit volume per second. In traversing an elementary volume of unit area and length  $dx$ , the colliding electrons produce an amount  $dn$  of new ions per second which is proportional to  $n_1$ , the number of electrons entering this volume per second, and the length  $dx$ . The proportionality constant is Townsend's first ionization coefficient  $\alpha$ . Thus, if recombination and diffusion are neglected and if  $\alpha$  is assumed constant throughout the region under consideration

$$dn = (\alpha n_1 + q_i) dx \quad (C-4)$$

If  $n_{o1}$  is the number of electrons emitted at the negative point (at  $x = 0$ ) by cosmic or artificial irradiation, integration of equation (C-4) gives

$$n_1(x) = n_{o1} e^{\alpha x} + \frac{q_i}{\alpha} (e^{\alpha x} - 1) \quad (C-5)$$

Since  $\alpha \approx 10$  for  $E/p = 60$  volts/centimeter at 760 mm Hg (Reference 6, page 150), there follows that for  $x \gg 0$  the term  $e^{\alpha x} \gg 1$ . Hence equation (C-5) can be reduced to

$$n_1(x) \approx \left[ n_{o1} + \frac{q_i}{\alpha} \right] e^{\alpha x} \quad (C-6)$$

Equation (C-5) is the electron current density in the units of electrons per second per square centimeter at an arbitrary position in the gaseous discharge. No consideration of secondary emission of electrons is made in obtaining this expression. In order to obtain the condition for corona onset, this expression must be modified

to give the electron current density when secondary emission is considered. This modification involves replacing the quantity  $n_{01}$  in equation (C-5) by its equivalent,  $n_c$ , when secondary emission is present (Reference 6). Let

$n_a$  = number of electrons reaching anode per unit area per second,

$n_{02}$  = number of electrons per unit area per second emitted from negative point due to cosmic rays, et cetera,

$q_i$  = ions per unit volume per second formed in inter-electrode space due to cosmic rays, et cetera,

$n_c$  = total number of electrons per unit area per second emitted from negative electrode due to cosmic rays, et cetera and to secondary emission, and

$c$  = distance from negative electrode to anode.

Then,  $n_a - n_c$  = number of positive ions formed in the atmosphere and

$$n_c = n_{02} + \gamma(n_a - n_c) \quad (C-7)$$

$$n_c = \frac{n_{02} + \gamma n_a}{1 + \gamma} \quad (C-8)$$

The quantity  $n_c$  is the equivalent of  $n_{01}$  when secondary emission is considered and replaces it in the expression for electron current density at any position  $x$  in the discharge equation (C-6). Therefore, with secondary emission considered, the electron current density at the anode is

$$n_a = (n_c + \frac{q_i}{\alpha}) e^{\alpha c} \quad (C-9)$$

Replacing  $n_c$  by using equation (C-8) gives

$$n_a = \left[ \frac{n_{02} + \gamma n_a}{1 + \gamma} + \frac{q_i}{\alpha} \right] e^{\alpha c} \quad (C-10)$$

Removing  $n_a$  from the right hand member of equation (C-10) we have

$$n_a = \frac{\left[ n_{02} + \frac{q_i}{\alpha}(1 + \gamma) \right] e^{\alpha c}}{1 - \gamma e^{\alpha c} + \gamma} \quad (C-11)$$

The total current density in gaseous discharge equals the sum of the positive ion and electron current densities. The law of current continuity states that total current density in any gaseous discharge is constant for any position in the discharge when steady state conditions exist. Therefore, the total current density equals the electron current density  $n_a$  (multiplied by  $e$ , the electron charge) at the position in the discharge where the positive ion current is zero.

This point is the anode. Therefore,

$$J_t = n_a e = \frac{e \left[ n_{02} + \frac{q_i}{\alpha}(1 + \gamma) \right]}{\gamma e^{\alpha c}} e^{\alpha c} \quad (C-12)$$

where  $J_t$  = total current density before breakdown and

$e$  = electronic charge.

The quantity  $\gamma$  has been neglected in comparison to

$$\gamma e^{\alpha c}$$

in the denominator of equation (C-11). Equation (C-12) is of practical use in predicting magnitudes of pre-breakdown discharge current.

It indicates that selecting the electrode material for proper  $\gamma$  can increase discharge current from the electrode.

The denominator of equation (C-12) gives the condition for negative corona onset. The condition is that the current density  $J_t$  increase without limit. This occurs if the denominator of equation (C-12) goes to zero, that is if

$$\gamma e^{-\alpha c} = 1 \quad (C-13)$$

Equation (C-13) implies that corona commences at that value of electrical field which causes at least one new electron to be emitted from the negative electrode when it is bombarded by the positive ions present in an avalanche. The discharge is termed "self-sustaining" at this stage. The exact value of electric field at which corona occurs in air at constant temperature and pressure is a function of corona electrode radius of curvature. A low corona threshold value is very favorable in that discharge current is then larger at a given electrode voltage as shown by equation (D-50). Reference 19, page 153, gives data on the corona onset values of electric field for negative points with radii ranging from 0.00023 inches to 0.018 inches at different point to plane spacings (gap lengths). By the term "plane" we make reference to the infinite plane approximation to the aircraft fuselage discussed in Section B. Thus, the aircraft fuselage is considered to have the same effect on the corona current of the electrostatic discharger system as the plane used in the laboratory experiments described in Reference 19. The data show that, for a given point radius of curvature, the corona onset electric field has become unchanging with respect to change in gap length for gap lengths greater than approximately 3.14 inches (8 centimeters). Also, for a given gap length, the value of corona onset electric field decreases as radius of curvature increases approaching a constant value,  $E_D = 62$  kilovolts/centimeter at a point radius of 0.018 inch for large gap lengths. The values of corona

onset electric field in this data were found by using the applied voltage and appropriate physical dimensions in the laboratory experiment in the expression for electric field at the corona point for hyperboloidal point and opposing plane geometry given by

$$E_D = \frac{2 V_C}{R_t + \ln\left(\frac{4C}{R_t}\right)} \quad (C-14)$$

where  $c$  = distance between corona point and plane,

$V_C$  = corona probe threshold voltage,

$R_t$  = radius of curvature of the point, and

$E_D$  = field intensity at the discharging electrode,

The preceding expression and data can be used to give data meaningful to the electrostatic discharger system. The basis of applicability is that as discussed above, for gap lengths greater than 3.14 inches (8 centimeters) the value of corona onset electric field is constant for a given corona point radius. Thus, the potential  $V_C$  with respect to the aircraft necessary for onset of the corona current in the electrostatic discharger system can be calculated from the relationship (C-14) using the value of point to plane (fuselage) spacings,  $c$  (greater than 3.14 inches), the corona point radius of curvature  $R_t$ , and the value of onset electric field  $E_D$  appropriate to gap length (given in the data from Reference 19). Figure 3 shows curves resulting from such computations for  $V_C$ . These curves give the relationship between negative corona threshold voltage and electrode tip radius of curvature for three different distances between aircraft and corona electrode. The symbols used in these curves (squares, et cetera) indicate the values of point radius of curvature and point-fuselage spacing for which values of  $V_C$  were actually

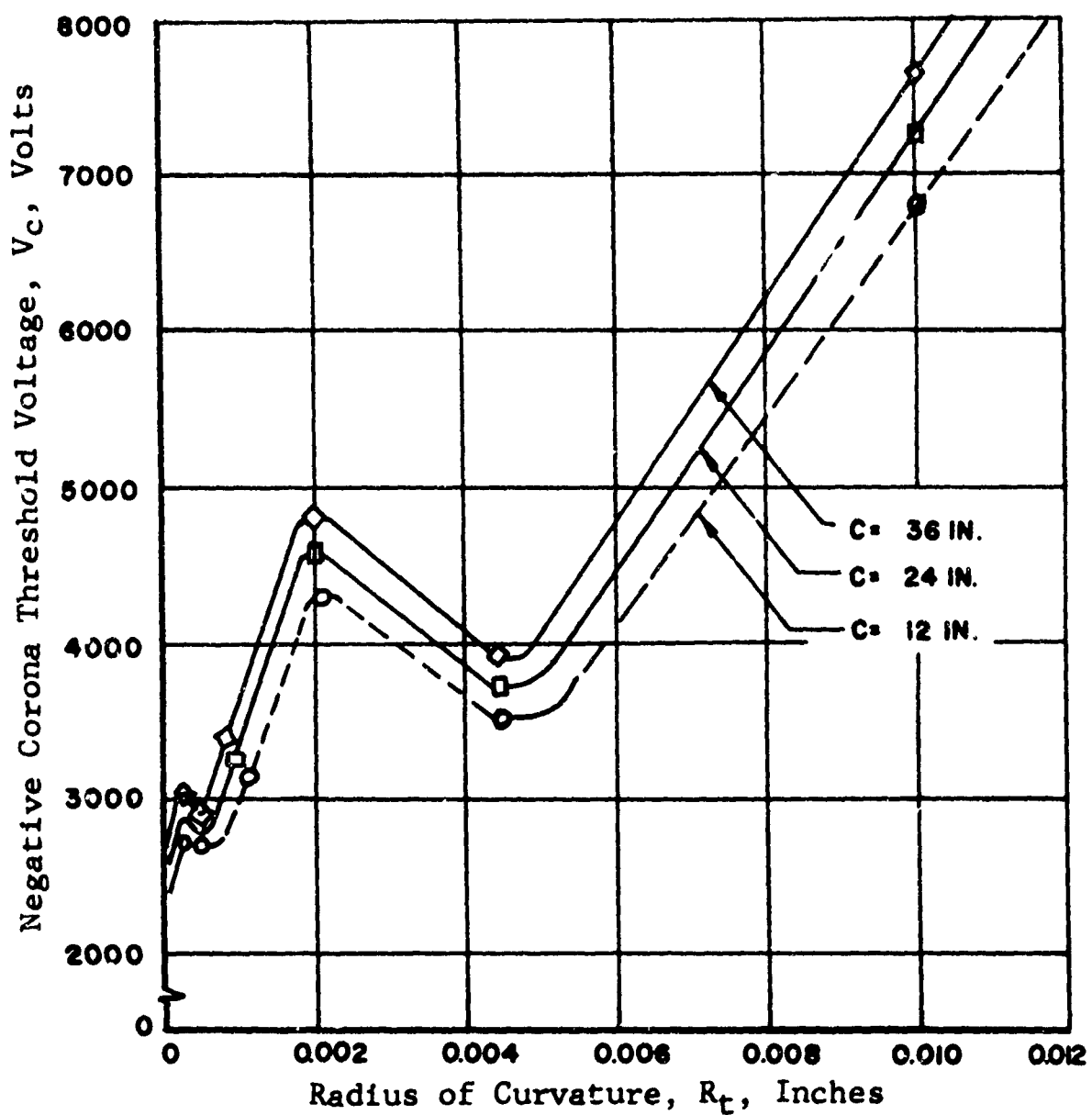


Figure 3. Minimum Negative Probe Voltage Required for Initiating Corona as a Function of Electrode Tip Radius and Spacing from Aircraft.

calculated. The four maximum and minimum points on the curves result from the fact that field intensity  $E_p$  varies nonlinearly both with  $R_t$  and  $c$ , as indicated in Reference 19, page 153. The curves indicate that the corona threshold voltage is approximately independent of corona electrode tip radius for values of radius between 0.002 and 0.006 inch. Corona point deterioration because of positive ion bombardment (sputtering) makes it impossible to maintain a tip radius of less than 0.001 inch in actual operation (Reference 18). Thus, referring to Figure 3, the best corona electrode tip radius of curvature is between 0.002 and 0.006 inch, and is therefore a noncritical dimension.

### Corona Discharge

The term "corona discharge" actually signifies glow discharge on a curved electrode (Reference 9). Thus, corona physics is that of the familiar glow discharge. This type of gaseous conduction is characterized by low voltage and is independent of current density. Another characteristic of the corona discharge is a voltage drop concentrated over a short distance from the cathode about equal in magnitude to the breakdown potential of air. This concentration of voltage drop is caused by the tendency of the positive ions to drift toward the cathode and form a virtual anode there. Microscopic investigation of the voltage drop region shows it to be composed of a series of relatively light and dark regions called the Aston dark space. The positive column, a region of small voltage gradient due to small net space charge and masked cathode, comprises the remainder of the discharge. In normal operation of the discharger system, the corona discharge is confined to a region only a few electrode tip radii, (Reference 18). The discharge region extends to the aircraft only if arc-over occurs.

The phenomena occurring in corona discharge as the negative electrode voltage is increased from the corona threshold value are described as follows. The rate of change of potential with distance ceases to be a constant as the effects of space charge caused by ionization begin

to set in. As voltage is increased further, the cathode fall of potential becomes a constant determined by the electrode material (approximately 300 volts), and the current emitting area of the electrode increases causing discharge current to increase. The current density, however, remains constant at this stage. The remainder of the corona electrode high voltage developed by the system is dropped from the periphery of the corona discharge to the aircraft surface. With further increase of negative voltage, the current density begins to increase and arcs or streamers occur between the electrode and the virtual anode. Destruction of the discharge electrode follows because of positive ion bombardment and heavy current loading (Reference 18).

The ionization processes in the atmosphere cause the presence of electrons, positive oxygen ions, negative oxygen ions, positive nitrogen ions, and ionizing photons as constituents of the discharge. The primary processes are



In closed spaces, the nitrogen gaseous compounds are noxious. The corona current in the atmosphere has a unique pulsed characteristic (Reference 12) because of the presence of an electronegative gas (oxygen). Neutral molecules of electronegative gases have a great affinity to attach electrons in regions of small E/p, that is, where electrons have small velocities. The resulting heavy immobile negative ions accumulate and eventually choke-off the corona current momentarily, thereby causing the pulsed characteristic. Corona current in pure nitrogen and hydrogen gases which are not electronegative, are much greater in magnitude and are not pulsed. These gases, once the steady state is reached, have space charge distributions depending on position only. For the Trichel corona current pulse, named after its discoverer, the space charge distri-

bution depends on both position relative to the corona electrode and time. The characteristics of the Trichel pulse are important because the system discharge current is the time average of the pulsed current.

The steps in the negative pulse formation are as follows. A random positive ion due to cosmic radiation is accelerated toward the negative electrode. Initially, the field is high enough to accelerate the ion to sufficient energy to cause the emission of a secondary electron when it reaches the electrode. This electron produces a dense cloud of positive ions by the Townsend avalanche mechanism as it is repelled from the negative electrode. This slow moving positive ion space charge reduces the field of the negative electrode at its outer periphery where it is already weak due to distance from the electrode. Consequently, the repelled electrons lose energy rapidly and form negative ions by attachment to neutral oxygen molecules. The accumulation of these negative immobile ions reduces the field which had been drawing the positive ions to the electrode. It is this effect which tends to choke off the current.

The decelerated positive ions proceed without producing further ionization to the electrode where they form the current pulse and contribute to the discharge of the negatively charged aircraft. By the time the last few positive ions approach the electrode, the negative heavy ion space charge may have been cleared sufficiently by the viscous downwash forces, that the field is high enough to cause another repetition of the pulse. It is unlikely that free electrons attach to form ions in regions of the discharge where they have an average energy corresponding to that causing excitation and ionization, that is, where  $E/p$  exceeds 90 volts per centimeter per millimeter Hg, since detachment of electrons from the neutral oxygen molecules occurs at these values of  $E/p$ .

The corona electrode performance is improved due to its location in the rotor downwash region. The airstream tends to prevent accumulation of the heavy negative ions around the electrode. The corona current is therefore greater since less choke-off occurs.

Parameters of the negative corona current pulse such as pulse repetition rate, duration, and rise time depend on the following:

1. Electrode configuration
2. Electrode-aircraft separation
3. Material of the electrode
4. Environmental conditions
5. Applied voltage

The bases for the above statement are the following considerations which also indicate how these conditions affect the corona current pulse parameters. By definition the average corona current is the net amount of charge entering the corona point divided by the time interval required for this charge to enter the point. In the pulsed nature of negative corona current as qualitatively described in the preceding paragraph, a fixed amount of charge enters the point in a specific small time interval (pulse duration time). (In general, for voltages near corona onset, the Trichel pulses are somewhat random and irregular. As the electrode voltage is increased, the pulses become regular.) Thus, in mathematical terms, the average corona current,  $I$ , is given (Reference 16) by

$$I = F_r \cdot em \quad (C-17)$$

where  $I$  is corona discharge current,

$F_r$  is pulse repetition rate (reciprocal of pulse duration time),

$m$  is number of ions involved in one current pulse, and

$e$  is electronic charge.

The quantity  $m$  is given in the Townsend avalanche mechanism theory (Reference 19) as

$$m = n_0 e^{\int_0^c \alpha dx} \quad (C-18)$$

where  $n_0$  is the number of electrons emitted at the negative corona electrode,

$\alpha$  is Townsend's first ionization coefficient, and

$c$  is distance from negative corona electrode to virtual anode.

The integral,  $\int_0^c \alpha dx$ , is not exactly evaluable because of the complicated dependence of  $\alpha$  on  $x$  through the relationship of  $E$  with  $x$  (References 19 and 11), and recalling that  $\alpha = pf(E/p)$ , see equation (C-3). The latter relationship differs from the basic  $E$  versus distance relationship given in Section B because of the effects of space charge due to atmospheric ionization. The exact relationship can be obtained through the differential equations of Section D, page 56. The literature (Reference 11) describes the exact equations as solvable by computer (differential analyzer). In practice, the number of ions involved in a pulse is obtained through graphical integration of the current pulse shape to determine the included area which equals the amount of charge (number of ions multiplied by electronic charge,  $e$ ).

The faster the ions involved in the pulse move, the shorter will be the time duration of the pulse and the greater the repetition rate,  $F_r$ , will become. Ion velocity is determined by electrical field intensity,  $E$ , being directly proportional to it with constant of proportionality,  $k_1$ , the ion mobility (discussed in Section D, page 51). Thus, the following equation can be written

$$F_r = k_r v = k_r k_i E \quad (C-19)$$

where  $v$  is ion velocity,

$F_r$  is pulse repetition rate,

$k_r$  is the constant of proportionality between  $F_r$  and  $v$ ,

$k_i$  is the ion mobility constant of proportionality, and

$E$  is electric field intensity.

Hence, equation (C-17) can be rewritten as follows:

$$I = A n_{OA} e^{\int_0^c \rho s(E/p) dx} k_r k_i E e \quad (C-20)$$

where  $A$  is current emissive surface area of corona electrode,

$n_{OA}$  is number of ions emitted at corona electrode per unit area, and

$p$ ,  $k_r$ ,  $k_i$ ,  $E$ ,  $e$ , and  $x$  have been defined previously.

Equation (C-20) shows quantitatively the way in which the five conditions listed on page 23 influence corona current. Electrode configuration determines  $A$  and the value of  $E$  at any point in the discharge. Electrode aircraft separation determines the value of  $E$  at points in the discharge in accordance with the considerations in Section B. Material of the electrode affects  $n_{OA}$  through the mechanism of secondary emission from the electrode. Also, the material of the electrode affects its configuration in consequence of durability considerations. Environmental conditions determine  $p$  and, through temperature, affect ion mobility. Applied voltage partially determines  $E$  (refer to equations on page 56). Since an increase of the applied potential accelerates the Trichel pulse cycle, the pulse repetition rate,  $F_r$ , is increased with an increase of applied voltage. The number of ions

involved in one current pulse,  $m$ , remains constant as the negative electrode voltage is increased from the corona threshold value. Hence, near onset, negative corona current is directly proportional to applied voltage. This holds over a considerable range in voltage but eventually, as electrode voltage is increased, there is a departure from the linear current. This indicates a decrease in the number of ions,  $m$ , per pulse. A Trichel pulse repetition rate of 10 megacycles/second has been observed before the applied voltage reached the arc-over point and 100 megacycles/second is theoretically possible (Reference 19). The number of ions  $m$  for a point of 0.2-mm radius is about  $10^9$  ions. Thus, application of equation (C-17) indicates that a current of 1 microamp corresponds to a pulse repetition rate of 6 kilocycles per second. A current of about 50 microamps can be obtained for an applied voltage of 40 kilovolts in a point-plane arrangement with a gap of about 6 inches. The near proximity of the plane to the corona electrode increases the corona current significantly because of the resulting increased field strength at the electrode as explained in Section D. Of course, current going to the infinite plane is analogous to discharge current returning to the aircraft. An actual discharger system permitting this to occur would not be acceptable. The action of the airstream tends to prevent this by diverting this current from the aircraft, if the airspeed is sufficiently high, as, for example, for a very high speed aircraft. For helicopters, however, the maximum available airspeed is not sufficient to permit the use of this approach for the design of the corona probe. Reference 14 gives values of rise time and duration for the negative Trichel pulse. Typical values at atmospheric pressure are risetimes of 12 nanoseconds and pulse duration of 30 nanoseconds for a 0.015-inch radius electrode tip at 30 kilovolts.

#### POSITIVE CORONA CHARACTERISTICS

Two types of positive corona, depending on atmospheric characteristics and applied voltage, may occur. These are burst pulse corona similar to the Trichel pulse, and streamer (or brush) corona (Reference 19). They differ in appearance markedly. By considerations similar to those used in finding the negative corona onset criterion, the condition for intermittent burst pulse corona may be derived as

$$\beta f_p e^{\int_0^c \alpha dx} = 1 \quad (C-21)$$

The significance of quantities in this expression are discussed below. Here as in the negative corona case,

$$e^{\int_0^c \alpha dx}$$

is the number of ions in an electron avalanche. In the case of positive corona, the avalanche is due to ionization by a naturally occurring trigger electron as it is accelerated toward the corona electrode. The ions which have provided the electrons for the avalanche constitute a positive space charge when the avalanche has entered the positive electrode. Similar to the Trichel pulse phenomenon of negative corona discharge, this positive space charge causes burst pulses of corona discharge current. The burst pulse duration can be from tens to hundreds of microseconds. In contrast to the negative corona mechanism, the appearance of new electrons is not due to secondary emission, but due to photoionization. This occurs during the last portion of the path traveled by the avalanche electrons which, before entering the positive electrode, create a number of photons of high energy ultraviolet light by impacts with atoms. The number of photons produced is proportional to

$$e^{\int_0^c \alpha dx}$$

and is therefore given by

$$f_p e^{\int_0^c \alpha dx}$$

in which  $f_p$  is a constant of proportionality. A fraction,  $\beta$ , of these photons escape absorption and create electrons in the gas within a distance  $c$  from the electrode by photoionization. Any of these photoelectrons can cause a new avalanche which will perpetuate the process. The onset criterion in equation (C-21) signifies the production of at least one new electron to start a new avalanche and therefore self-maintenance of the discharge.

Streamers occur when the positive ion charge density is large enough to act as an extension of the positive electrode. Under these conditions, electrons are drawn to the positive ion charge density. They ionize air molecules causing more positive space charge. Thus the streamer extends itself considerably into the gap as a luminous conducting filament. Streamers appear only at low currents or at high currents just before breakdown. Consequently, the current over most of the gap between the point and plane consists of randomly spaced burst pulses.

Figure 4 shows curves of positive corona threshold voltage as a function of radius of curvature. These curves were calculated similarly to those for negative corona threshold, that is, the point-plane approximation was used. The remarks made for negative corona with respect to dimension of electrode tip also apply for positive corona.

#### COMPARISON BETWEEN POSITIVE AND NEGATIVE CORONA

Consideration of the positive and negative corona onset conditions with the values of  $\gamma$  and  $\beta f_p$  appropriate to air ( $\gamma \approx 10^{-3}$ ,  $\beta f_p \approx 10^{-4}$ ) applied seems to indicate that the negative Trichel pulse onset voltage is lower than the positive burst pulse onset voltage (Reference 12). It would also be expected that the negative onset voltage which depends on  $\gamma$  would be sensitive to the electrode material and condition while the positive onset voltage would depend on the gas only. In air, however, the two thresholds are markedly close together. The thresholds are about the same, even when corona electrodes of different metals such as platinum, copper, and zinc are used. The

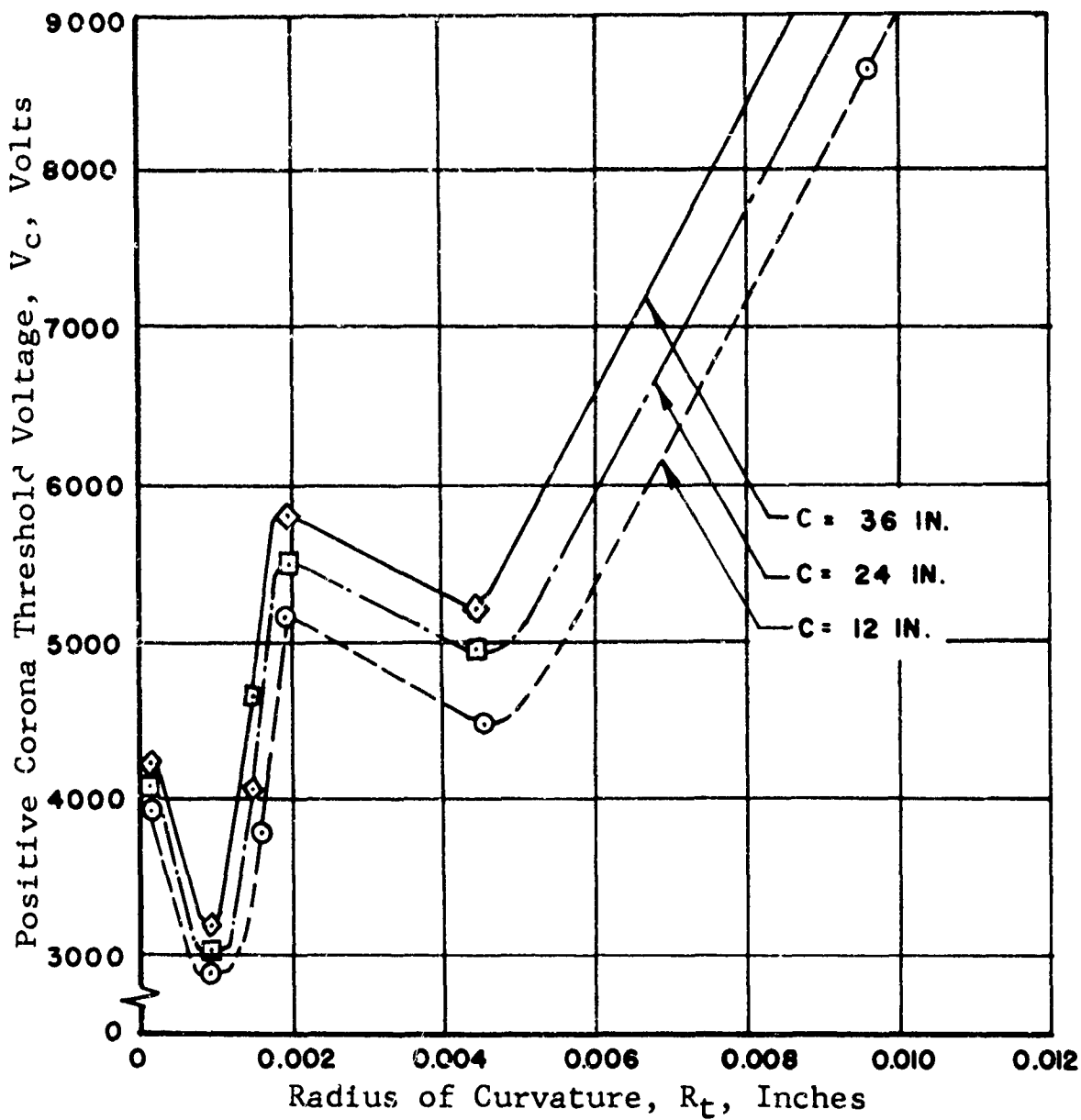


Figure 4. Minimum Positive Probe Voltage Required for Initiating Corona as a Function of Electrode Tip Radius and Spacing from Aircraft.

explanation for the equality in view of the difference in  $\gamma$  and  $\beta f_p$  is that  $\gamma$  is decreased for the negative electrode by the effects of surface absorption of oxygen becoming fortuitously equal to  $\beta f_p$  for air.

A difference in the magnitudes of positive and negative corona current for the same electrode voltage has been observed (Reference 5). This is caused by a difference in the clearing time of the choke-off space charge which affects the pulse shape and, therefore, the average current. The rate of clearing is approximately twice as rapid with the negative electrode since the electrons traverse part of the gap as electrons and attach to ions later. Also, the mobility of negative ions in air is 30 per cent greater than that of positive ions due to its smaller mass to area ratio. The number of ions,  $m$ , in streamers and burst pulses is of the same order of magnitude as in the negative Trichel pulses. The pulse repetition rate,  $F_r$ , however, is reduced some 50 percent for positive corona current because of the longer clearing time. Consequently, near onset for the same conditions, the negative corona currents in air are of the order of twice as great as the positive corona currents. For both polarities an Ohm's law regime exists near onset.

#### CORONA DISCHARGING CURRENT IN STILL AIR

An equation for the magnitude of the corona discharging current is presented in Reference 2, page 32, as will be further discussed in Section D (equation D-50). In still air, this equation reduces to

$$I = AC V_a (V_a - V_c) \quad (C-22)$$

where A and C are constants for a particular corona probe-fuselage configuration. Figure 5 presents experimental data of corona current at zero airspeed measured during Contract DA 44-177-AMC-T(3) and from other data obtained by this contractor. For a value of  $AC = 0.83 \times 10^{-14}$  and  $V_c = 2000$  volts, equation (C-22) provides the following comparison with the experimental data.

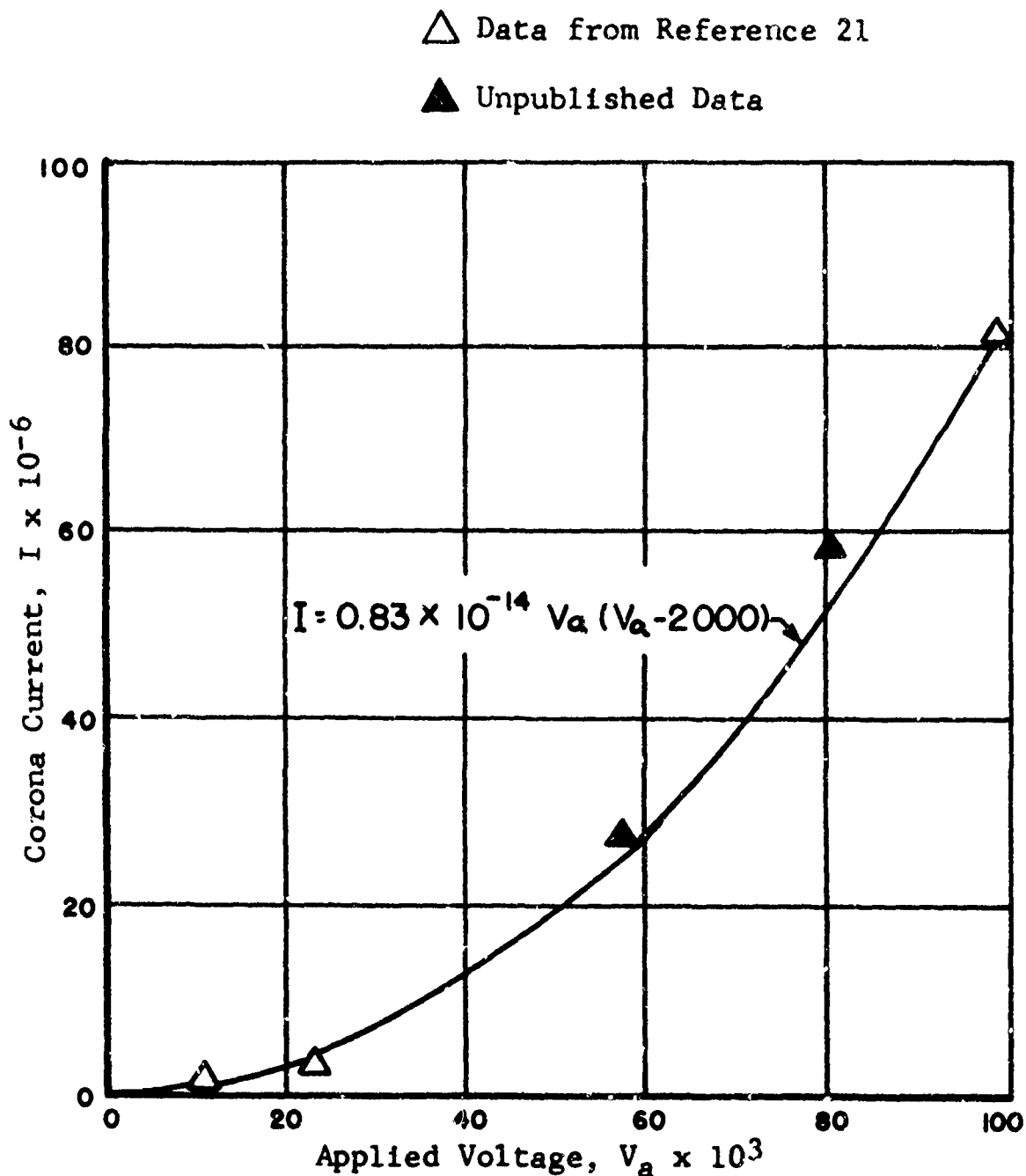


Figure 5. Corona Discharging Current in Still Air.

TABLE I

Theoretical		
$V_a \times 10^{-3}$ Volts	$I \times 10^{-6}$ amps	$I \times 10^{-6}$ amps
0	0	0
1	-0.0083 (maximum negative value)	0
2	0	0
10	0.664	1
23	4.0	4.0
100	81.5	78.0

It should be noted that whereas experimentally, and obviously physically, the current is zero up to the corona threshold  $V_c = 2000$  volts, the theoretical expression shows negative currents for values of  $V_a < V_c$ .

The reason for this discrepancy is that the assumptions made in formulating equation (C-22) do not consider the discontinuity that the threshold voltage represents in the basic physical process of corona action. The discrepancy, however, is seen to result in a practically insignificant small value of negative current.

## SECTION D: CALCULATION OF CORONA CURRENT IN MOVING AIR

Derivation of an expression for corona current serves to make evident the various factors influencing discharge current magnitude. This information enables design of the corona electrode for maximum discharge current capability. Such optimization makes possible light, small discharger systems. The derivation is based on the corona theory given in the preceding section. This section first gives a general description of the current discharge from a corona electrode mounted on a helicopter under in-flight conditions. Detailed descriptions of the factors influencing the discharge follows. The section includes a derivation of an equation for corona current involving these factors. The ion trajectory is also stated.

### AIRCRAFT CHARGE DISSIPATION FROM THE CORONA ELECTRODE

The discharger system applies a large voltage difference between the corona electrode and the aircraft surface in order to create large electrical field strength at the electrode. This field strength causes ionization of the surrounding atmosphere and, consequently, causes the presence of positive ions and electrons near the electrode (Section C). Since the polarity of the electrode is that of the electrostatic charge picked up by the aircraft, the particles (positive ions or electrons) attracted to the electrode neutralize the aircraft charge. The trajectory of the repulsed particles is of importance for the following reasons. Any accumulation of repulsed particles near the corona electrode constitutes a space charge which limits the magnitude of discharge current and reduces the ionizing electric field. In addition, any return of repulsed particles to the aircraft reduces discharger system effectiveness by reducing the net discharge current. The trajectory of the repulsed particles is determined by the total force exerted on them. Because of their small mass, the ions will travel in the direction of the total vector force at any point. This force is the vector sum of the electrical force and the viscous air-stream or wind force on the particles at any instant. That is,

$$\vec{F}_t = \vec{F}_e + \vec{F}_w \quad (D-1)$$

where  $\vec{F}_t$  = vector total force on the repulsed particles at any instant,  
 $\vec{F}_e$  = electric force vector on the repulsed particles, and  
 $\vec{F}_w$  = vector viscous wind force at any instant.

The two components of the total force are discussed in detail in this section.

In summary, the phenomena determining the magnitude of corona discharge current and which, therefore, must be considered in the derivation are as follows:

1. Electric field of specific electrode geometry influenced by a distribution of space charge.
2. Ionization of air by this electrical field.
3. Space charge density buildup resulting from this ionization as a function of time and position.
4. Effect of wind and electric field on space distribution and ion trajectories.

#### EFFECT OF AIRCRAFT ON DISCHARGER ELECTRICAL FIELD

The electrical component,  $\vec{F}_e$ , in equation (D-1) is significantly affected by the electrically conductive objects in proximity to the corona electrode. The discharger system can be considered to operate completely isolated from all objects except the aircraft structure since the discharger functions only during flight. The

proximity of a conductive object connected to the airframe will increase the recirculated current percentage. and hence decrease the probe effectiveness.

The field distribution near a corona probe has been analyzed in Section B. The analysis did not include the effect of space charge density due to the motion of ionized particles. This density is, however, very small except in the zone very near to the corona probe, and in this zone, the effect of the space charge was discussed in Section C. Hence, the model of the corona discharge in air is a blend between the corona discharging phenomenon taking place in the zone near the probe followed by an ionic distribution determined by the electrostatic and viscous forces predominant in zones relatively far away from the probe tip. The current distribution in these zones will be analyzed later in this section.

#### COMPONENT OF ION MOTION DUE TO ELECTRICAL FIELD OF DISCHARGER

It is instructive to compare ion motion under actual discharger operating conditions, that is, in the atmosphere, with their motion in a vacuum. In the latter case the ions travel along the electric field lines without interference from the air molecules with an increasing velocity  $v$  given by Newton's second law. The differential equation which must be solved to obtain  $v$  is

$$\mathbf{F}_e = m_i \frac{d\mathbf{v}}{dt} = e \mathbf{\bar{E}} \quad (D-2)$$

where  $\mathbf{F}_e$  is force vector on ion equation (B-9),

$m_i$  is ion mass,

$\mathbf{\bar{v}}$  is vector ion velocity, and

$\mathbf{\bar{E}}$  is vector electric field caused by discharger system, as shown in equation (B-7).

The presence of the atmosphere, however, slows up the motion of ions in an electric field because of the repeated collisions with neutral molecules which result

in kinetic energy losses. At each impact the ion loses much of its velocity in the field direction. After a large number of collisions have occurred, the ion has an average or drift velocity in the field direction which is directly proportional to  $E$  and inversely proportional to the atmospheric density. This drift velocity is constant for a given  $E$  rather than increasing as it does in vacuum. The drift velocity divided by the electric field is therefore a constant. This ratio is termed "mobility" and depends only on gaseous composition and density (Reference 6). Thus, in still air, ions in the atmosphere still travel along the lines of force but with a constant velocity. Assuming zero initial velocity, the expression for ion velocity in atmosphere is

$$\vec{v} = k_i \vec{E} \quad (D-3)$$

where  $\vec{v}$  = ion velocity,

$k_i$  = mobility constant of ions, and

$\vec{E}$  = field strength.

Since the electric field lines of the discharger system extend between the corona electrode and the aircraft surface, there is a definite tendency in still air for discharge current to return to the aircraft. If it were not for the airstream past the discharger electrode, special measures, such as the application of insulative coatings to the aircraft, would have to be considered. The wind prevents return current by exerting a force on the ions which diverts them from the electric field lines.

#### COMPONENT OF ION MOTION DUE TO AIRSTREAM PAST DISCHARGER ELECTRODE

The ion motion caused by the airstream is completely determined if the viscous wind force on the ion and the initial ion velocity are known. If the viscous force on the ions is much larger than the electrical

force their trajectory is along the lines of viscous force; if not, the ion trajectory is along the vector resultant of the viscous and electrical force.

The magnitude of viscous force on a body in an airstream is given by conventional aerodynamic theory as a function of the coefficient of drag. This coefficient is a function of the shape of the object and the reynolds number of the airstream. Reference 10 suggests this technique can be used to determine the magnitude of viscous force on the ions of the corona discharge current if the ion is considered a small rigid sphere. This reference gives drag coefficient information for spheres with diameter as small as  $2 \times 10^{-3}$  centimeter. The diameter of the ions of the discharge current are much smaller than this value when first formed. However, rapid attachment of these ions by larger particles of the air augments the particle diameter by several orders of magnitude. Thus, the use of formulas in Reference 10 to calculate an approximate drag coefficient for the ions of the discharge current is a justified extrapolation.

Accordingly, the viscous force exerted by the airstream on the ions of the aircraft discharging current is given by

$$\vec{F}_w = C_D q_r S \quad (D-4)$$

where  $q_r$  = dynamic pressure caused by airstream,

$S$  = ion projected area (assumed spherical),

$C_D$  = coefficient of drag, and

$\vec{F}_w$  = viscous airstream force.

For practical use of equation (D-4), equations for the quantities appearing in it must be given. These are:

$$q_r = 1/2 (\rho_a w^2) \quad (D-5)$$

$$C_D = 27 / (Re)^{.84} \quad (D-6)$$

$$Re = \frac{wd}{\nu} \quad (D-7)$$

Applying these relationships to equation (D-4) gives a more useful expression for viscous force. This is

$$\vec{F}_w = \frac{1}{2} C_d \rho_A w^2 s = 338 \pi \nu^{.84} (wo)^{1.16} \rho_A \quad (D-8)$$

In the preceding four equations,

$\rho_A$  is airstream density (free stream),

w is airstream speed,

Re is reynolds number,

d is diameter of ion, and

$\nu$  is kinematic viscosity of airstream.

Equation (D-8) displays the dependence of viscous force  $\vec{F}_w$  on environmental conditions. It is seen that viscous force increases nearly linearly with increase of airstream speed and kinematic viscosity. The effects of temperature and pressure on viscous force are contained in the direct proportionality of  $\vec{F}_w$  to free stream density  $\rho_A$ . Since  $\rho_A$  is directly proportional to ambient pressure and inversely proportional to temperature, viscous force,  $\vec{F}_w$ , increases as ambient pressure increases if temperature remains constant. Also the viscous force decreases with increase of atmospheric temperature if ambient pressure remains constant.

#### ION TRAJECTORY DUE TO VISCOUS AND ELECTRICAL FORCE OF DISCHARGER SYSTEM

By use of equations (D-1), (B-9), and (D-8), the forces acting on an ion can be computed.

$$\begin{aligned}
 \vec{F}_t &= \vec{F}_e + \vec{F}_w \\
 &= \frac{q v_p R_t}{2c^2} \left( \frac{2 - \frac{R_t}{c}}{1 - \frac{R_t}{c}} \right) \left\{ \frac{\frac{R_t}{c}}{\left[ \left( \frac{R_t}{c} \right)^2 + \left( \frac{c-h}{c} \right)^2 \right]^{3/2}} - \frac{\frac{R_t}{c}}{\left[ \left( \frac{R_t}{c} \right)^2 + \left( \frac{c+h}{c} \right)^2 \right]^{3/2}} \right\} \vec{n}_1 \\
 &\quad - \left[ \frac{\frac{c-h}{c}}{\left[ \left( \frac{R_t}{c} \right)^2 + \left( \frac{c-h}{c} \right)^2 \right]^{3/2}} + \frac{\frac{c+h}{c}}{\left[ \left( \frac{R_t}{c} \right)^2 + \left( \frac{c+h}{c} \right)^2 \right]^{3/2}} \right] \vec{n}_2 \\
 &\quad + \left\{ 3.38 \pi \rho_A v^{0.84} (wD)^{1.16} \right\} \vec{n}_1
 \end{aligned} \tag{D-9}$$

Typical values obtained from equation (D-9) for  $\vec{F}_e$  and  $\vec{F}_w$  are shown in Figure 6 and Figure 7 for  $h=c$  and  $h = c/2$ , respectively. In these figures, the following values were utilized:

$$\begin{aligned}
 R_t &= 0.002 \text{ inches} \\
 v_p &= 50,000 \text{ volts} \\
 q &= 1.6 \times 10^{-9} \text{ coulombs} \\
 c &= 24 \text{ inches} \\
 d &= 1.43 \times 10^{-8} \text{ inches} \\
 w &= 720 \text{ inches/second}
 \end{aligned}$$

As seen from Figures 6 and 7, near the corona electrode the electric component of force,  $\vec{F}_e$ , on the ions is much larger in magnitude than the viscous airstream component  $\vec{F}_w$ . Thus, the ion trajectory near the electrode will be in the direction of the electric field lines, that is, the trajectory has the direction of  $\vec{F}_e$  at points near the corona electrode.

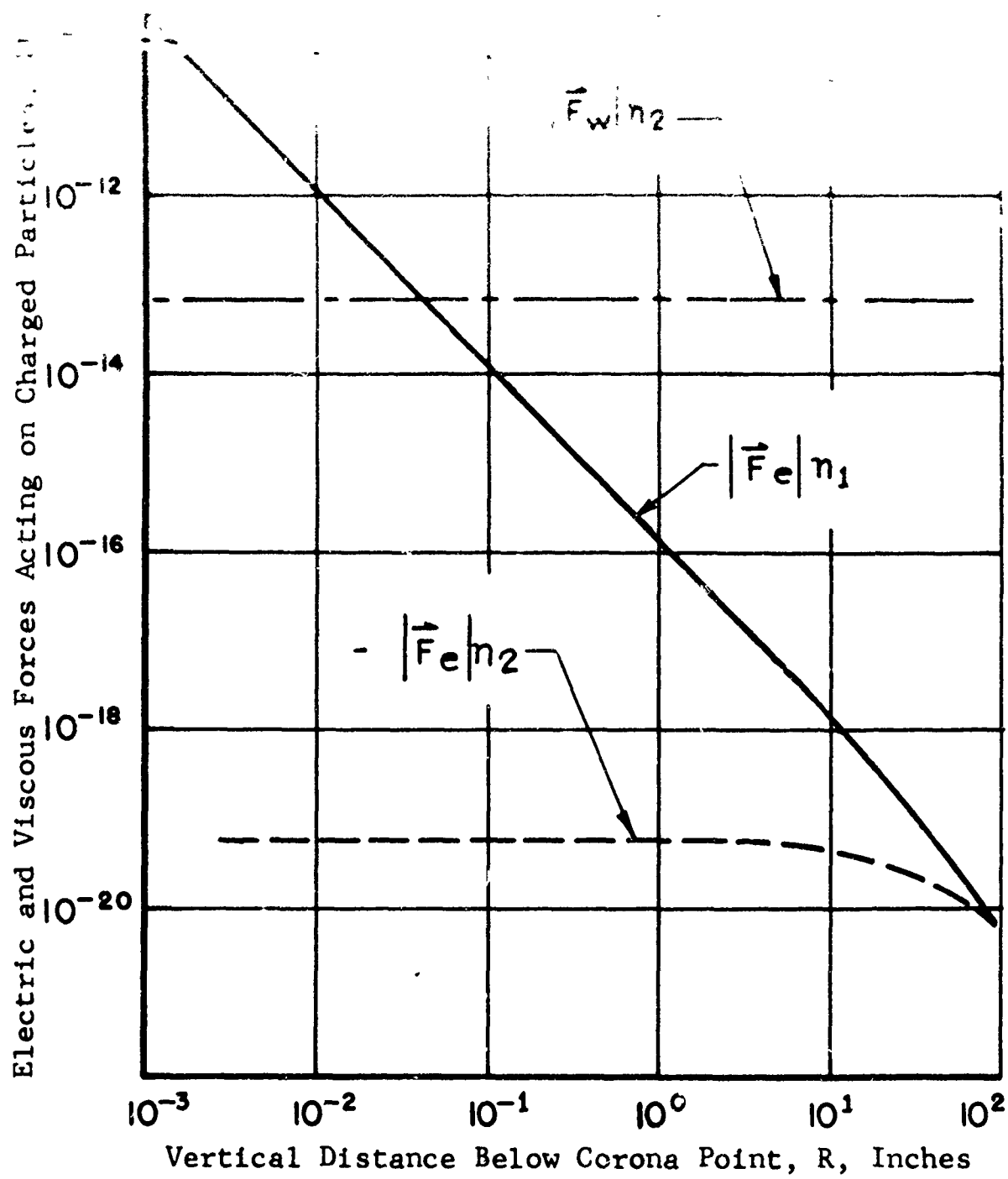


Figure 6. Force Vectors Acting on a Charged Particle  
at  $h = c$ .

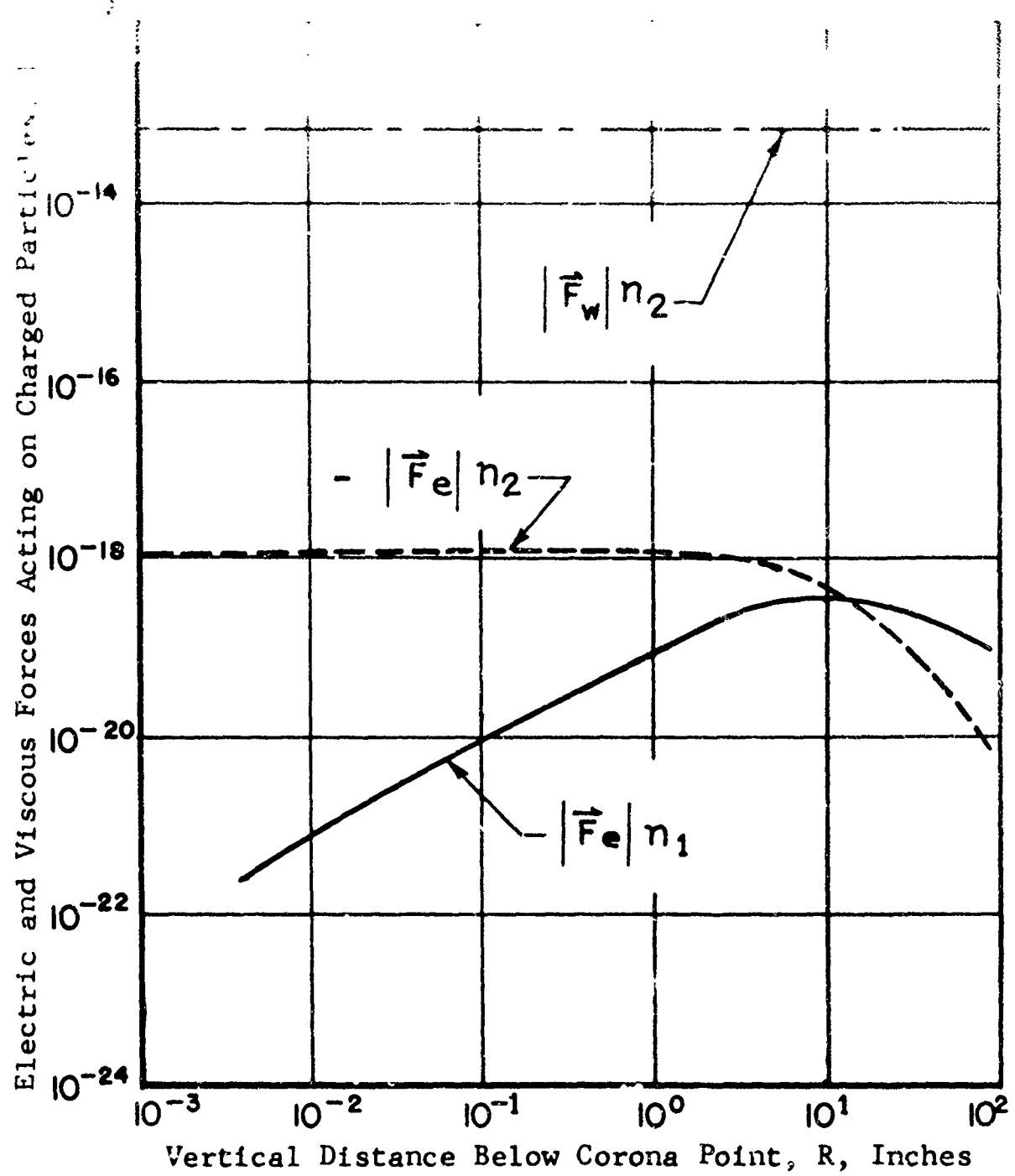


Figure 7. Force Vectors Acting on a Charged Particle  
at  $h = c/2$ .

Equation 1 shows that as the distance increases, the direction of the total force,  $\vec{F}_t$ , becomes quite small in comparison to the viscous airstream component which remains relatively constant and, hence,  $\vec{F}_t$  has essentially the direction of the downward velocity vector,  $\vec{F}_w$ .

### EFFECT OF ELECTRODE TIP RADIUS

For a discharge electrode of point geometry, there is an optimum radius of curvature which represents a compromise between the factors described below. Because of deterioration, however, it is impossible to maintain this optimum radius. The operating conditions determined by tip radius and the significance of these conditions to system performance are discussed in the following paragraphs.

#### Magnitude of Field Intensity in the Vicinity of the Corona Electrode at a Given Voltage

The field strength for given applied voltage and ambient charge density about the corona electrode is completely determined by the electrode configuration. Corona current occurs only when the field strength is equal to or greater than a value of approximately 30 kilovolts per centimeter (Reference 19). The corona current pulse repetition rate,  $F_r$ , increases as the field strength increases and, therefore, according to equation (C-17), the corona current also increases with field strength. Small radius of curvature of the corona electrode tip will minimize the voltage required to produce a given field strength since the field increases as the radius of curvature of the tip decreases. The voltage required for corona onset depends on the electrode tip radius in the manner shown in Figures 3 and 4. Magnitude of corona current increases as the corona onset potential decreases in accordance with equation (D-50).

#### Extent of the High Field Region Around the Electrode Tip

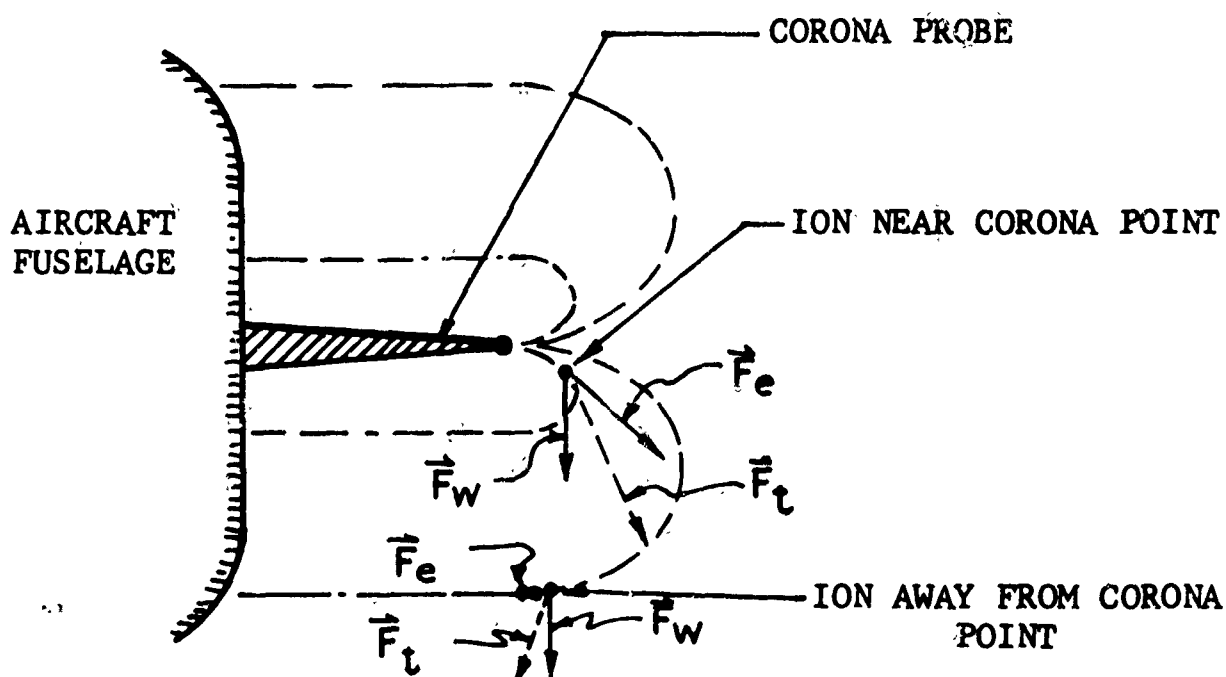
As shown in equation (C-17), the corona current level is proportional to the number of ions in one pulse. A large value of  $m$  will result only if the extent of high field region about the corona electrode is appreciable. The extent of high field region increases as the radius of curvature of the tip decreases.

### Surface area of Point

Since current density in corona discharge is constant over a wide range of voltage, the current is directly proportional to the point surface area. Too small a point is very prone to performance degradation due to positive ion bombardment (sputtering). Electrode tip deterioration by sputtering results in a tip with a much increased radius of curvature and, consequently, an increased surface area (Reference 18). Too large a surface area may mean a loss in field intensity.

### Effect of Wind

The presence of wind produces viscous forces on the ions. In the close vicinity of the probe tip, these forces are substantially smaller in magnitude than the electrostatic forces, which in that zone are necessarily very high to produce ionization. Hence, the resultant force vector is essentially equal to the electrostatic force vector. This implies that the effects on the probe performance of tip radius and the airspeed are essentially negligible. Vector representation of the forces acting on the ions in the vicinity of the corona tip is shown in the sketch below.



## FORMULATION OF THE CORONA CURRENT EQUATIONS

The theoretical procedure for formulation of the system of equations which would have to be solved for determination of the exact expression for corona current is now discussed. The resulting equations are very complex and exact mathematical solutions require techniques which are beyond the scope of this program. Formulation of the equations, however, does have the value of clarifying the physical mechanisms which occur and thus provide guidelines for sound corona probe design and experimental optimizing modifications.

The formulation of the equations is achieved by mathematically adding up the changes in the number of charged particles in an infinitesimal volume at a given location in the corona discharge during an infinitesimal time interval due to the various physical mechanisms to obtain the overall rate of change for each particle. Since there are three different particles involved (electrons, positive ions, and negative ions due to electron attachment to oxygen molecules), three equations are necessary. The fourth and final equation is the well-known poisson electrostatic equation relating the number of charged particles per unit volume to electrical field. An exact solution for this system of equations would give the concentration of each of the particles and the electrical field as a function of time and location.

The physical mechanisms described in the equations, a particle population balance diagram for an infinitesimal volume, and derivation of the equations are given below. A general expression showing how the value of corona current could, in theory, be obtained from the solution of the above four equations will also be given.

Assumptions are made as described in the following derivation.

1. For each electron generated by ionization, a positive ion is generated.
2. Positive oxygen and nitrogen ions have the same diffusion, recombination, and mobility constants.
3. Positive ions do not produce ionization because of their relatively large mass.
4. Although electron and positive ions are generated by the same ionizing event,  $n_1$  is not equal  $n_2$  because of electron attachment to form negative ions.
5. No combination of positive and negative ions occurs.
6. Molecules of the atmosphere are single ionized.

The physical mechanisms of importance in determining electrostatic discharger system corona current follow.

#### Particle Generation Due to Ionization By Electrons

In advancing a unit distance in the atmosphere in the direction of the electrical field, a single electron creates  $\alpha$  (Townsend's first ionization coefficient discussed in Section C, page 13) new electrons and positive ions. The increase in charged particles  $dn$  caused by  $n_1$  electrons in advancing a distance  $dx$ , is given by the relation

$$dn = \alpha n_1 dx \quad (D-10)$$

The rate of electron increase due to this mechanism in the infinitesimal volume (of unit cross section) is

$$\frac{dn_1}{dt} = \alpha n_1, \frac{dx}{dt} = \alpha n_1 \vec{v} \quad (D-11)$$

By using equation (D-3), there follows

$$\frac{dn_1}{dt} = \alpha n_1 k_1 |\vec{E}_1| \quad (D-12)$$

where  $n_1$  is number of electrons located within the infinitesimal volume, that is, electron concentration.

If the assumption is made that one positive ion results from each electron generated in this mechanism, the contribution to the positive ion population due to ionization by electrons is

$$\frac{dn_2}{dt} = \alpha n_1 k_1 |\vec{E}_2| \quad (D-13)$$

where  $n_2$  is the number of positive ions in the infinitesimal volume. The viscous forces acting on the electron can be considered in the preceding two equations by use of an "effective" electric field. This is accomplished by assuming  $E$  to consist of the actual electric field,  $\vec{E}_T$ , plus an equivalent electric field,  $\vec{E}_w$ , which expresses the viscous effects on the particular ion. That is

$$\vec{E} = \vec{E}_T + \vec{E}_w \quad (D-14)$$

where

$$\vec{E}_w = \vec{F}_w/e$$

$$\vec{F}_w = C_D q r S / e$$

Since  $S$  is very small for electrons, the effects of viscous forces in contributing to ionization are negligible in comparison to the effects of electric forces. Viscous forces are important in determining distribution of ions through other mechanisms as described below. Ionization by electrons is not a factor in causing negative ions.

### Particle Generation Due to Volume Ionization

Here, reference is made to the contribution made by naturally occurring ambient ionization normally always present and due to cosmic rays and natural radioactivity. This mechanism is represented mathematically by the symbol  $q_i$ , where  $q_i$  equals natural time rate of ionization. The term  $q_i$  is the rate of positive ion generation as well as electron generation through natural causes. This stems from the fact that for each electron produced, one positive ion is produced, that is, the molecules of the atmosphere are being single ionized by these natural causes. Volume ionization does not contribute to negative ion generation.

### Particle Depletion Due to Recombination

In this mechanism, electrons reunite with positive ions causing the loss of the two particles from their respective populations and the possible emission of light in the process. The number of individual recombinations during an incremental time,  $dt$ , for a region in which  $n_1$  and  $n_2$  are uniform concentrations of particles per unit volume is

$$dn = -\alpha_r n_1 n_2 dt \quad (D-15)$$

where, by definition,  $\alpha_r$ , is the coefficient of recombination (Reference 19, page 20). The quantity  $\alpha_r$  depends on pressure and temperature since these conditions affect the number of positive and negative ions present and available for recombination in a given volume of air. For air at  $0^\circ\text{C}$  and 760 mm pressure,  $\alpha_r$  is  $1.71 \times 10^{-6}$  cubic centimeter/second (Reference 6, page 99).

### Particle Depletion Due to Diffusion

Wherever the concentration of charged particles varies from point to point in a gas, that is, where a concentration gradient exists, there will be a flow of these particles from regions of high concentration to regions of lower concentration. Thus, diffusion produces a de-ionizing effect in high concentrated regions and an ionizing effect in the adjacent regions of lower ion concentration. If  $n_1$  is the number of charged particles at a given point, the

concentration gradient is  $\nabla n$ , where  $\nabla$  is the differential operator of vector calculus. The rate of increase or decrease into or out of the small volume being considered in the particle population balance is directly proportional to the divergence of the concentration gradient, that is,  $\nabla \cdot \nabla n_i$  or  $\nabla^2 n_i$ . Thus rate of particle increase or decrease due to diffusion is given mathematically by

$$\frac{dn_i}{dt} = D_i \nabla^2 n_i \quad (\text{for } i = 1, 2, \text{ and } 3) \quad (\text{D-16})$$

where  $D_i$  is the constant of proportionality or diffusion constant.

The value of  $dn/dt$  may be positive or negative corresponding to ionization or de-ionization (depletion), respectively, according to whether the net gradient over the surfaces of the infinitesimal volume (the vector divergence) is positive or negative (Reference 11, page 189). The diffusion coefficient  $D_i$  is related to the mobility constant  $k_i$  for a given ion by

$$D_i = \frac{k_i \rho}{N e} \quad (\text{D-17})$$

where  $N$  is the number of molecules per cubic centimeter at pressure  $p$  (Reference 19, page 30).

The ion mobility constant is discussed below in connection with the physical mechanism of particle generation or depletion due to electrical charge motion induced by the electric field.  $D_i$  is inversely proportional to pressure and, for atmosphere with water content, directly proportional to the 1.75 power of temperature.

#### Negative Ion Generation Due to Electron Attachment

As mentioned in the description of the events occurring in corona discharge (Section B), the attachment phenomena causes the pulsed nature of the discharge. In this phenomenon, electrons are attached by neutral molecules of the oxygen of the atmosphere when these electrons reach regions of the discharge where  $E/p$  has been reduced to 20 volts/centimeter/ mm Hg or less (Reference 19, page 28). The coefficient of attachment,  $\zeta$ , which is the average

number of collisions the electron must make before attaching itself to a neutral atom, is not related to any property of the atmosphere, except to its electronegative (tendency to capture electrons due to O<sub>2</sub> content) character. If  $\tau$  is the mean time for an electron to become attached to a molecule of the atmosphere, then the rate of electron depletion from the infinitesimal volume, or alternatively, the rate of negative ion generation, is given by

$$\frac{dn_z}{dt} = \frac{n_i}{\tau} \quad (D-18)$$

The value of  $\tau$  for air at 0°C and 760 mm Hg is  $6.3 \times 10^{-7}$  seconds (Reference 6, page 97). There is a dependence of  $\tau$  on temperature and pressure, since  $\tau$  equals the coefficient of attachment divided by the number of electron collisions per second with air molecules, the latter being temperature and pressure dependent.

#### Particle Generation or Depletion Due to Electrical Charge Motion Induced by the Electric Field

From basic electric theory (Reference 8, page 187) the rate of charge buildup or decrease (depending on algebraic sign of the final result),  $dq/dt$ , in the infinitesimal volume under consideration is given

$$\iint_{S_a} J_i \cdot d\vec{s}_a = -\frac{dq}{dt} \quad (\text{for } i = 1, 2, 3) \quad (D-19)$$

where  $\vec{J}_i$  is current density of charged particles, and  $d\vec{s}_a$  is infinitesimal area element.

If  $\rho_i$  represents the volume charge density at the location of the infinitesimal volume under consideration

$$-\frac{dq}{dt} = -\frac{d}{dt} \iiint_{V_a} \rho_i dV_a = \iint_{V_a} \vec{J}_i \cdot d\vec{s}_a \quad (D-20)$$

Using stokes theorem,

$$\iint_{S_a} \vec{J}_i \cdot d\vec{s}_a = \iiint_{V_a} \vec{\nabla} \cdot \vec{J}_i dV_a = \iiint_{V_a} \left( \frac{d\rho_i}{dt} \right) dV_a \quad (D-21)$$

where the negative sign and differentiation with respect to time has been brought under the triple integral sign. Thus, the following equation for rate of change of volume charge density is obtained by equating integrands in the preceding equal triple integrals:

$$\vec{\nabla} \cdot \vec{J}_i = - \frac{d\rho_i}{dt} \quad (D-22)$$

The preceding equation will be applied to each of the three types of charged particle involved in the corona discharge in deriving the discharge equations. For electrons,

$$\vec{J}_e = - n_e e \vec{v}_e \quad (D-23)$$

The minus sign in the preceding equation is due to convention. Also,

$$\rho_e = n_e e \quad (D-24)$$

Thus, the rate of change of electron population in the infinitesimal volume due to field induced charge motion,  $dn_1/dt$ , is given by

$$-e \vec{\nabla} \cdot n_e \vec{v}_e = -e \frac{dn_1}{dt} \quad (D-25)$$

or

$$\vec{\nabla} \cdot n_e \vec{v}_e = \frac{dn_1}{dt}$$

The electron velocity can be replaced immediately by one of the quantities which the system of equations to be derived should involve and, also, give knowledge of. This quantity is the electric field intensity  $\vec{E}$ . The relationship to be used to enable this replacement is equation (D-3). Thus,

$$\frac{dn_1}{dt} = \vec{\nabla} \cdot n_1 k_1 \vec{E}, \quad (D-26)$$

Again  $\vec{E}_1$  can be considered to consist as the sum of the actual electric field and an equivalent electric field to represent the viscous force effects.

The mobility constant for ions,  $k_1$ , is independent of  $E/p$  over a wide range of  $E/p$  values provided that the speed of drift in the field is appreciably less than the velocity of thermal agitation. The product of electron mobility and pressure,  $k_1 \times p$ , in air is approximately constant from an  $E/p$  value of 0 to 22 volts/centimeter/mm Hg. The approximate value of the  $k_1 \times p$  product is

$$5 \times 10^{-5} \frac{\text{cm}}{\text{sec}} \frac{\text{mm Hg}}{\text{V/cm}} \quad (\text{Reference 19, page 35.})$$

For positive ions,

$$\vec{j}_2 = n_2 e \vec{v}_2 \quad (D-27)$$

where in this case,  $v_2$  is the positive ion velocity and  $e$  is positive ion charge (equal to that of an electron because the air molecule has been deprived of one electron in forming the positive ion).

The signs in the preceding equation are such that positive ion current density is in the same direction (not the opposite direction as in the case of electrons) as the ion velocity in accordance with convention. Also,

$$\rho_2 = n_2 e \quad (D-28)$$

Thus, the rate of change of positive ion population in the infinitesimal volume due to field induced charge motion,  $dn_2/dt$ , is given by

$$e \vec{\nabla} \cdot n_2 \vec{v} = -e \frac{dn_2}{dt} \quad (\text{D-29})$$

or

$$\vec{\nabla} \cdot n_2 \vec{v}_2 = -\frac{dn_2}{dt}$$

The positive ion velocity can be replaced as in the case of electrons by the total electric field intensity  $\vec{E}_2$  experienced by the positive ion.  $\vec{E}_2$  contains an electric field component equivalent to the air stream viscous forces on positive ions. For positive ions, this viscous force term may not be negligible. Using the ion mobility constant for positive ions,

$$\vec{v}_2 = k_2 \vec{E}_2 \quad (\text{D-30})$$

Thus,

$$\frac{dn_2}{dt} = \vec{\nabla} \cdot n_2 k_2 \vec{E}_2 \quad (\text{D-31})$$

The mobility constant for atmospheric (dry) positive ions (singly charged) at 0°C and 760 mm Hg is 1.36 centimeters/second/volt/centimeters (Reference 6, page 38). For negative ions (those resulting from the attachment of electrons by air molecules due to their electronegative property and which, by causing the pulsed nature of corona discharge as described elsewhere in this report, play a significant role in electrostatic discharger operation),

$$\vec{J}_3 = -n_3 e \vec{v}_3 \quad (\text{D-32})$$

Again, the negative sign in the preceding equation is due to the definition of current density in terms of positive charge where here negative charge is being considered. Also,

$$J_3 = n_3 e \quad (\text{D-33})$$

Thus, the rate of change of electron population in the infinitesimal volume due to field induced charge motion,  $dn_3/dt$  is given by

$$-e \vec{\nabla} \cdot n_3 \vec{v}_3 = -e \frac{dn_3}{dt} \quad (D-34)$$

or

$$\vec{\nabla} \cdot n_3 \vec{v}_3 = \frac{dn_3}{dt}$$

Replacing  $\vec{v}_3$  by  $k_3 \vec{E}_3$ , as before, where  $k_3$  is the mobility constant for negative ions and  $\vec{E}_3$  is the total electric field (contains a component  $\vec{E}_{w3}$ , equaling the electrical equivalent of the airstream viscous forces on the negative ion) gives

$$\frac{dn_3}{dt} = \vec{\nabla} \cdot n_3 \vec{v}_3 \quad (D-35)$$

For negative ions the viscous force term may not be negligible. The mobility constant for negative ions of intermediate size (smaller than "Langevin" ions) at 0°C and 760 mm Hg is of the order of  $7 \times 10^{-2}$  square centimeter/volt second (Reference 11, page 172).

For still smaller singly charged negative ions (nonclustered) at 0°C and 760 mm Hg, the mobility constant is 2.1 square centimeter/volt second (Reference 6, page 38). Figure 8 shows a gaseous ion particle balance for the infinitesimal volume under consideration applying all the ionization and de-ionization mechanisms described above. With the information summed up in this diagram, three equations involving the concentrations  $n_1$ ,  $n_2$ ,  $n_3$  of the three ions in the corona discharge will be written below. A fourth equation must be obtained which, in conjunction with the aforementioned three, will enable solution in theory for the four quantities  $n_1$ ,  $n_2$ ,  $n_3$ ,  $E_T$  at every point in the discharge. This equation is basically the well known poisson equation and can be derived from the gauss law of electrostatics (Reference 8, page 43) and vector analysis. This law states that the normal component of the electric displacement vector,  $\vec{P}_1$ , taken over the surface of any closed volume equals the net charge enclosed in that volume. As an equation, the gauss law takes the form

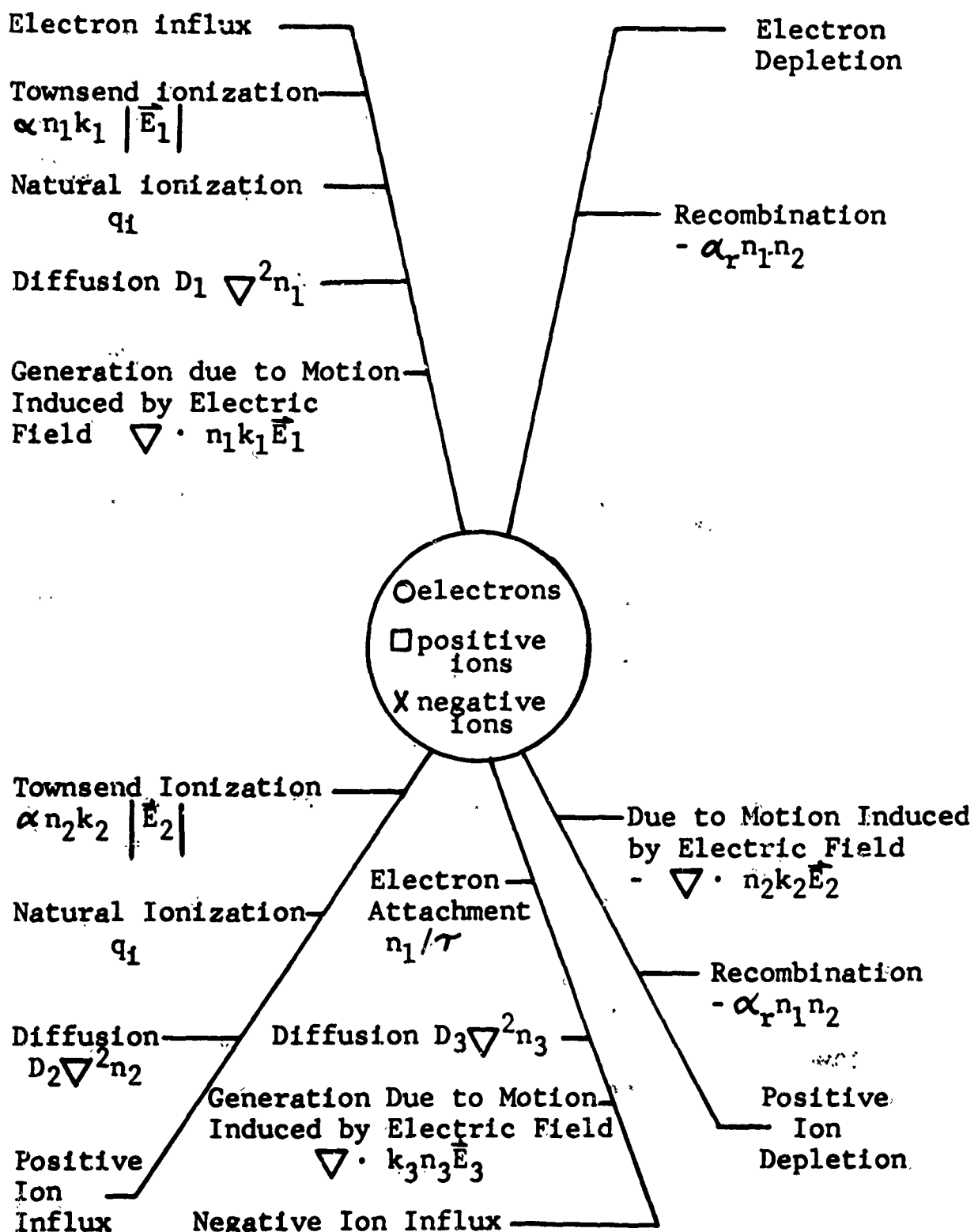


Figure 8. Particle Balance Diagram for Infinitesimal Volume.

$$\int_{S_a} \vec{\rho}_i \cdot d\vec{s}_a = q = \iiint_{V_a} \rho_i dV_a \quad (\text{D-36})$$

(for  $i = 1, 2, \text{ and } 3$ )

where  $dS_a$  is an element of surface area,

$q$  is net charge enclosed in the infinitesimal volume,

$\rho_i$  is net charge volume density of particles, and

$dV_a$  is an element of volume.

Using the divergence theorem, the preceding equation leads to

$$\iint_{S_a} \vec{\rho}_i \cdot d\vec{s}_a = \iiint_{V_a} \vec{\nabla} \cdot \vec{\rho}_i dV_a = \iiint_{V_a} \rho_i dV_a \quad (\text{D-37})$$

Since the limits of integration in the second and third members of the preceding equation are the same, the integrands must be equal. That is,

$$\vec{\nabla} \cdot \vec{\rho}_i = \rho_i \quad (\text{D-38})$$

Electric theory gives a relationship by which  $\vec{\rho}$  may be replaced in the preceding equation with one of the quantities to be found with the four equations, that is,  $E_T$ . This relationship is

$$\vec{\rho}_i = \epsilon_0 \vec{E}_T \quad (\text{D-39})$$

where  $\epsilon_0$  is electric permittivity of free space having a value  $8.85 \times 10^{-12}$  farad/meter in the MKS system.

In addition, the ion concentrations (number of ions per unit volume at an arbitrary location of the infinitesimal volume)  $n_1, n_2, n_3$  for the three ions of the discharge for which the equations are to be solved can be put in the equation by replacement of the quantity  $\rho$ . The relationship through which this is accomplished is

$$\rho = \rho_1 + \rho_2 + \rho_3 = e [n_2 - (n_1 + n_3)] \quad (\text{D-40})$$

where  $e$  is the electronic charge with a value of  $1.6 \times 10^{-19}$  coulomb in the MKS system.

Substitution of the preceding two equations in the equation immediately above involving  $P_i$  and  $\rho_i$  yields the required fourth equation,

$$\vec{\nabla} \cdot \vec{E}_T = \frac{e [n_2 - (n_1 + n_3)]}{\epsilon_0} \quad (D-41)$$

Referring to the particle balance diagram, Figure 8, in obtaining the time rate of change of concentration equation for each of the three ions (by adding up the contributions illustrated for the physical mechanisms described above) and restating the preceding equation gives for the four required equations:

$$q_i + n_i \alpha k_1 |\vec{E}_2| - \alpha_r n_1 n_2 + D_1 \nabla^2 n_1 + \vec{\nabla} \cdot (k_1 \vec{E}_1 n_1) - \frac{n_i}{\tau} = \frac{dn_i}{dt} \quad (D-42)$$

$$q_i + n_i \alpha k_1 |\vec{E}_2| - \alpha_r n_1 n_2 + D_2 \nabla^2 n_2 - \vec{\nabla} \cdot (k_2 \vec{E}_2 n_2) = \frac{dn_2}{dt} \quad (D-43)$$

$$\frac{n_1}{\tau} + D_3 \nabla^2 n_3 + \vec{\nabla} \cdot (k_3 \vec{E}_3 n_3) = \frac{dn_3}{dt} \quad (D-44)$$

$$\vec{\nabla} \cdot \vec{E}_T = + \frac{[n_2 - (n_1 + n_3)] e}{\epsilon_0} \quad (D-45)$$

In equations (D-42), (D-43), (D-44), and (D-45), the following definitions were utilized:

$n_1$  = electron concentration, that is, number of electrons per unit volume at an arbitrary point in the discharge

- $n_2$  = positive ion concentration  
 $n_3$  = negative ion concentration  
 $q_i$  = natural time rate of ionization due to natural causes such as cosmic rays, et cetera  
 $\alpha$  = Townsend's primary ionization coefficient, that is, the number of ion pairs formed per unit path length of travel of an ionizing particle (electron)  
 $\alpha_r$  = recombination coefficient of electrons and positive ions  
 $D_1, D_2, D_3$  = diffusion constants for each ion  
 $\tau$  = time for attachment of electrons to neutral oxygen molecules to form negative ions  
 $k_1, k_2, k_3$  = mobilities for each ion, that is, ratio of acquired velocity to electrical field  
 $\vec{E}_1, \vec{E}_2, \vec{E}_3$  = composite field or force per unit charge acting on each ion  
 $\vec{E}_T$  = that component of  $\vec{E}$  caused by electrical charge distribution  
 $\vec{E}_w$  = that component of  $\vec{E}$  caused by airstream or downwash  
 $e$  = charge of electron  
 $d\vec{S}$  = element of area of corona electrode tip  
 $i$  = corona current

Boundary conditions for the preceding four equations are that the solution for  $\vec{E}_T$  be such that the electric potential be constant over the geometry of the corona electrode

(the surface of an electrical conductor is an equipotential) and equal to the applied voltage. Also,  $\vec{E}_T$  must be equal to zero at infinity as must  $n_1$ ,  $n_2$ , and  $n_3$ . A similar but less general (for only two types of ion and one spatial dimension) set of equations is given in Reference 6, page 105, in the centimeter-gram-second system.

In theory (again computer methods would be needed for practical results), the solution of the four equations for  $n_1$ ,  $n_2$ ,  $n_3$ , and  $\vec{E}_T$  would make possible determination of the value of corona discharge current resulting from an application of the designated magnitude of voltage to the specified corona electrode under the given airstream conditions. The basic relationship for making this calculation is

$$i = \iint_{S_a} \vec{J}_i \cdot d\vec{s}_a \quad (D-46)$$

where  $i$  is corona discharge current.

By definition

$$\vec{J}_i = \rho_i \vec{v}_i$$

Since there are three types of charge passing through the surface of the corona electrode (the electrons, positive ions, negative ions), the preceding equation becomes a vector sum, each term dealing with one type of ion

$$\vec{J}_i = -\rho_1 \vec{v}_1 + \rho_2 \vec{v}_2 - \rho_3 \vec{v}_3 \quad (D-47)$$

where  $\rho_1$  is volume charge density for electrons, and

$\vec{v}_1$  is velocity of electrons, et cetera.

The first and third terms have minus signs because current is defined positive when in the direction of positive charge motion. Using the relationships

$$\rho_1 = n_1 e$$

$$\rho_2 = n_2 e$$

$$\rho_3 = n_3 e$$

and

$$\vec{v}_1 = k_1 \vec{E}_1$$

$$\vec{v}_2 = k_2 \vec{E}_2$$

$$\vec{v}_3 = k_3 \vec{E}_3$$

There follows that

$$i_a = c \iint_{S_a} (-n_1 k_1 \vec{E}_1 + n_2 k_2 \vec{E}_2 - n_3 k_3 \vec{E}_3) d\vec{s}_a \quad (D-48)$$

Evaluation of this expression by computer yields corona discharge current magnitude.

As mentioned before, the above equations are very difficult to solve. Hence, empirical equations have been utilized for obtaining the corona current. One such empirical equation for corona discharge current given in Reference 2, page 32 is

$$I = A (V + W) (V_a - V_c) \quad (D-49)$$

where  $V_a$  is applied voltage at corona electrode,

$V_c$  is corona threshold potential,

A is constant,

v is ion velocity,

w is wind velocity, and

I is average corona discharge current.

The constant A depends on ambient pressure, temperature, radius of curvature of corona electrode, and point-plane separation. No theoretical method has been found to determine the relationship of A and the above parameters and, hence, A must be determined from experimental data. The velocity of ions v is proportional to the electric field strength and, consequently, to the voltage applied to the electrode. Using equation (D-49),

$$\begin{aligned}
 v &= k_i E \\
 &= k_i C V_a \\
 &= C V_a
 \end{aligned}$$

This causes equation (D-49) to become

$$I = A(CV_a + W)(V_a - V_c) \quad (D-50)$$

Thus, the corona current voltage characteristics are of second degree for a given wind speed. Figure 9 shows typical experimental values of corona discharge current versus electrode voltage at two airstream velocities presented in Reference 5 and from additional flight test data obtained under Contract DA 44-177-AMC-114(T). The theoretical curve was obtained with  $A = 3.54 \times 10^{-12}$ ,  $C = 2.35 \times 10^{-3}$ , and  $V_c = 2000$  volts. It can be seen that good correlation exists between the limited experimental data available and theory.

Experimental Data from Reference 5.

Probe Point Radius 0.002 in

Corona Point Length 24 in

○  $W = 400 \text{ ft/sec}$

□  $W = 70 \text{ ft/sec}$

Unpublished Experimental Data Obtained under  
Contract DA 44-177-AMC-114(T)

△  $W = 70 \text{ ft/sec}$

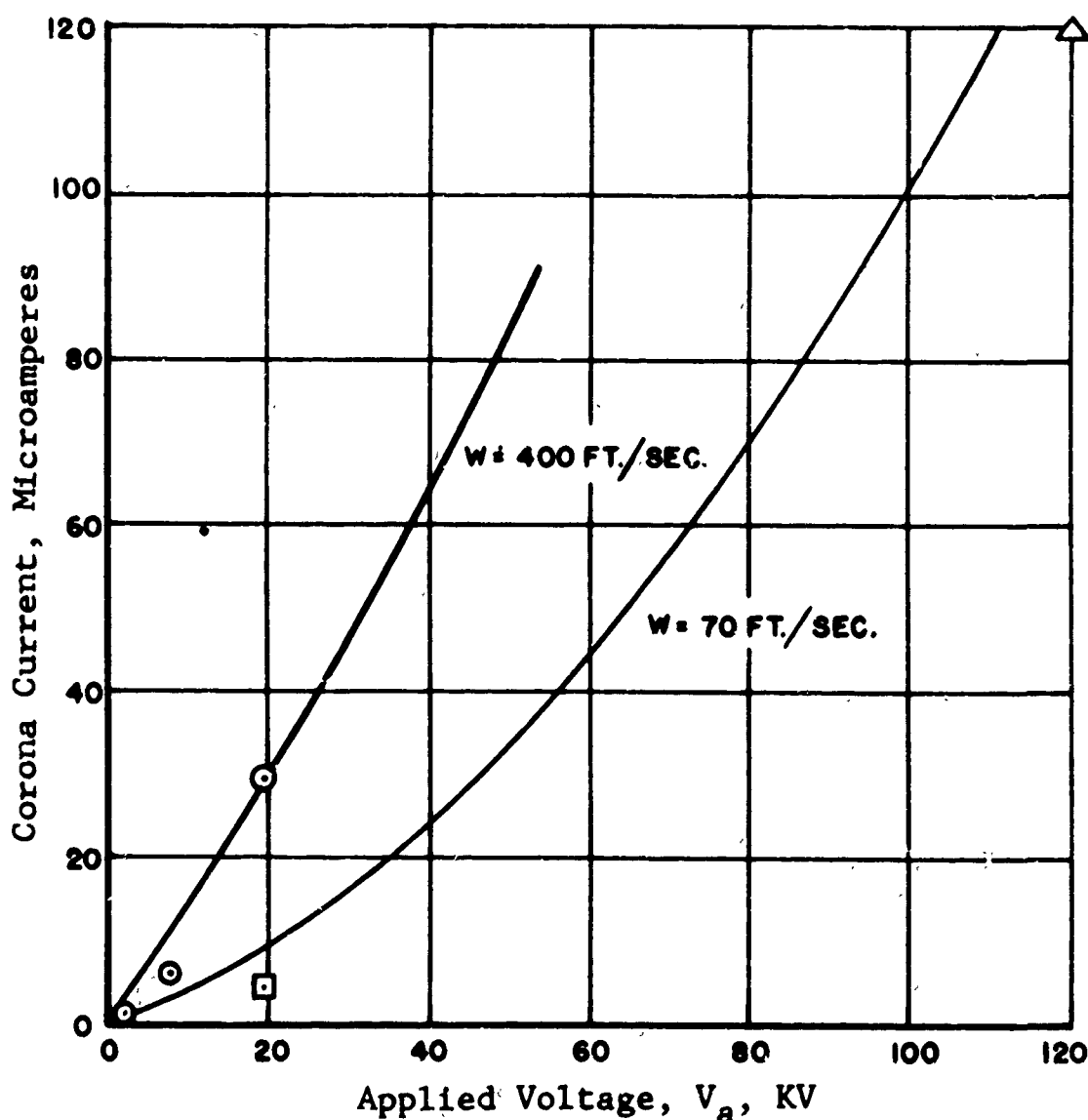


Figure 9. Corona Discharge Current Versus Electrode Voltage for Two Wind Speeds in a Typical Discharge System.

## SECTION E: EFFECTS OF ATMOSPHERIC CONDITIONS

### PRESSURE

The operating pressure for the corona probe equals the sum of the airstream dynamic pressure and the ambient atmospheric pressure. The pressure level is very important to system operation since the controlling field quantity at constant temperature is  $E/p$  as described in Section C. The dependence on  $E/p$  indicates that if pressure decreases by some factor, the field,  $E$ , necessary to maintain the same discharge current will be decreased by the same factor since an accordingly reduced  $E$  will keep the value of  $E/p$  constant. This is true only up to a certain limit of pressure reduction since corona discharge cannot occur in a vacuum. If the value of  $E/p$  is changed by variation of  $p$ , the first Townsend coefficient, described in Section C, will go through a maximum at  $E/p = 365$  volts per centimeter per millimeter Hg (Reference 6). Thus, there is a pressure for a given corona voltage and configuration at which corona current is a maximum. Some control of the airstream component of pressure to obtain a possible optimization of performance is possible by properly positioning the corona point in the airstream. Figure 10 shows the sensitivity of discharge current to change of pressure due to altitude.

### TEMPERATURE

The effects of temperature can be inferred from the gas theory equation.

$$N = \frac{P}{k_B T} \quad (E-1)$$

where  $P$  = pressure,

$N$  = number of molecules per unit volume,

$k_B$  = Boltzmann's gas constant, and

$T$  = absolute temperature.

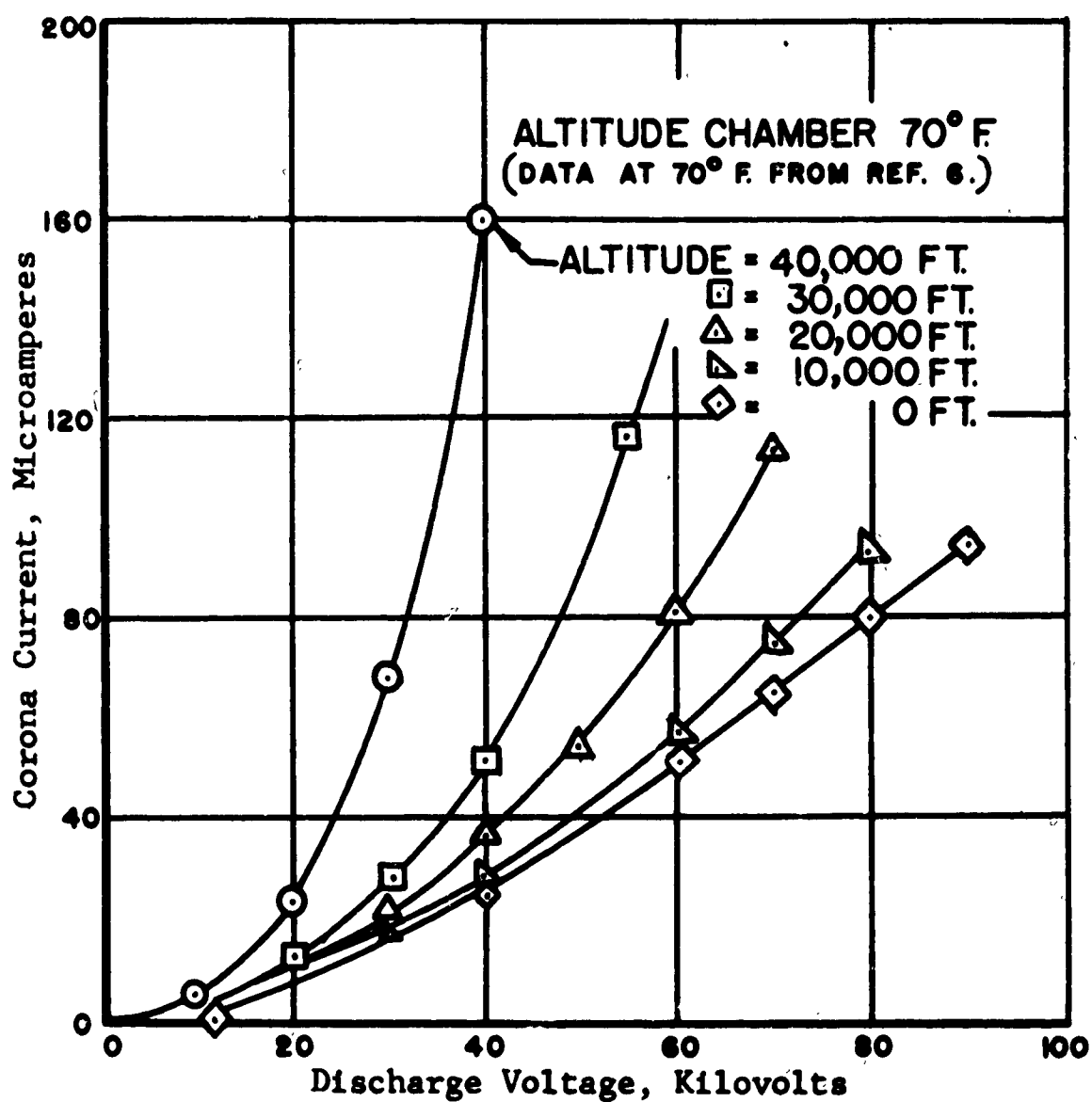


**Figure 10. Effect of Pressure Change Due to Altitude on Corona Electrode Performance.**

This equation implies that as temperature increases  $N$  decreases and therefore the number of molecules available for ionization decreases. This causes a loss in corona current. If temperature is increased substantially ( $4000^{\circ}\text{K}$ ), thermal ionization sets in and corona current may begin to increase with temperature (Reference 6).

#### MOISTURE

The presence of humidity in the air has a double effect on discharger performance. It prevents the aircraft from acquiring charge. Also, it inhibits the performance of the discharger electrode. Both these effects are due to the tendency of water molecules to capture charge. Thus, in humid regions, the collection of charge of both polarities into which an aircraft flies discharges it over its entire surface. Also, the operation of a corona probe in a high humidity atmosphere results in the formation of a moisture layer over the surface of the isolating supporting structure. This moisture layer presents an electrical path between the probe tip and the aircraft fuselage which results in an increased load of the electrical generator which maintains the probe potential. These generators are very high impedance devices and, hence, their terminal voltage drops due to the increased load. This voltage drop results in a decreased performance of the discharging systems.

#### PURITY

Contamination of the corona point by oil, grease, or tarnish will diminish corona current by reducing the second ionization coefficient for the point, that is, secondary emission is reduced.

SECTION F: INVESTIGATION OF CORONA PROBE PERFORMANCE  
IMPROVEMENT

Reduction of corona electrode voltage requirements would be a very significant contribution to electrostatic discharger system optimization. Reduced operating voltage would permit a more easily maintained, smaller, and lighter discharger system. Maximizing the magnitude of corona discharge current for a given corona electrode voltage makes possible the desired decrease in required operating voltage. This section investigates several possible approaches to the maximization of corona current.

THE RADIOACTIVE CORONA PROBE

Radioactive materials emit particles which ionize the surrounding air, making it conductive. These materials, therefore, have the ability to cause a certain amount of discharge if applied to an electrostatically charged aircraft. However, the amount of radioactive material required to achieve electrostatic discharge if radioactive materials alone are used is prohibitively large (Reference 2). The use of radioactive material as a method of improving the performance of the electrostatic discharger system corona electrode is conceivable. The possible improvements obtainable by use of radioactive probes operating at high voltages can best be obtained by appropriate experiments.

IRRADIATION OF CORONA ELECTRODE WITH ULTRAVIOLET LIGHT

Both this method and the use of radioactivity are based on the generation of an increased number of triggering electrons for the corona discharge. Without some special provision such as these, the magnitude of corona current is limited by the relatively small ionization level set by natural causes such as cosmic rays and radioactive traces. Ultraviolet radiation will emit photoelectrons from normal corona electrode materials such as steel (essentially iron) since the energy,  $E_{u.v.}$ , of a photon of ultraviolet light exceeds the work-function,  $W_f$ , of iron for photoelectric emission. The following calculation is the basis for this statement.

$$\begin{aligned}
 E_{u.v.} &= h_p f \\
 &= 6.624 \times 10^{-27} \text{ erg-sec} \times 10^{15} \text{ cycles/sec} \\
 &= 6.624 \times 10^{-12} \text{ erg} \\
 &= 4.16 \text{ electron volts} \tag{F-1}
 \end{aligned}$$

where  $h_p$  is planck constant,  $6.624 \times 10^{-27}$  erg-sec,  
 $f$  is ultraviolet light frequency,  $10^{15}$  cps, and  
 $E_{u.v.}$  is energy of ultraviolet light photon.

Reference 23, page 2656, indicates that  $W_f$  for iron is

$$W_f = 3.9 \text{ electron volts.} \tag{F-2}$$

The above calculations indicate that the ultraviolet photon energy is barely sufficient to produce electron emission from iron. Considering the losses to be expected due to impurities in the probe, et cetera, it is believed that the use of ultraviolet light for increasing corona probe performance is impractical.

#### COATING OF CORONA ELECTRODE WITH PHOTOEMISSIVE MATERIAL

If the corona electrodes are coated with materials especially selected for low photoelectric work function such as activated cesium, irradiation of the corona electrode with light in the visible range could result in performance improvement. Suitable experiments should be performed to determine the extent of these improvements.

#### OPERATION OF CORONA ELECTRODE IN ENGINE EXHAUST

In principle, an engine exhaust is a possible means of accomplishing alone or assisting a corona discharge system in removal of electrostatic charge from aircraft. This is due to the presence of ions in the hot gasses of the engine exhaust caused by the phenomenon of thermal ionization. These ions improve the performance of the corona electrode by contribution to the number of trigger electrons in a way similar to the mechanism of current enhancement by radioactivity.

Unfortunately, the practical use of engine exhaust ionization to improve electrostatic discharger system performance is very severely limited by the exhaust temperature requirements. The results of calculation using the basic equation of thermal ionization, Saha's equation (Reference 6), verify the excessive temperature requirements. Saha's equation for one component of the engine exhaust is

$$\frac{r^2}{1-r^2} p = 3.16 \times 10^{-7} T^{2.5} e^{-\frac{eV_i}{k_B T}} \quad (F-3)$$

where  $p$  is total pressure in atmospheres,

$T$  is the temperature of the exhaust in degrees, kelvin,

$eV_i$  is the energy required for ionization of the gas atoms in ergs,

$k_B$  is Botzman's constant, and

$r$  is fraction of atoms ionized in each mole of engine exhaust as it leaves engine.

We calculate the value of  $r$  for  $\text{CO}_2$ , a typical engine exhaust component (Reference 6) at the following conditions:

$P = 1$  atmosphere

$T = 2000^\circ\text{K}$  ( $3140^\circ\text{F}$ )

$V_i = 5.5$  volts.

Substituting values in Saha's equation,

$$\frac{r^2}{1-r^2} \times 1 = 3.16 \times 10^{-7} (2000)^{2.5} \times \frac{1.6 \times 10^{-19} \times 5.5}{1.38 \times 10^{-23} \times 2000} \approx 0 \quad (F-4)$$

therefore,

$$r \approx 0$$

The low value of  $r$  obtained even at elevated temperature demonstrates the nonfeasibility of corona probe performance improvement by the use of helicopter engine exhaust. The operating temperature of helicopter engine exhausts (Reference 21) is approximately 800°F. The temperature of jet engine exhaust is also too low for use in electrostatic discharger system performance improvement with jet aircraft.

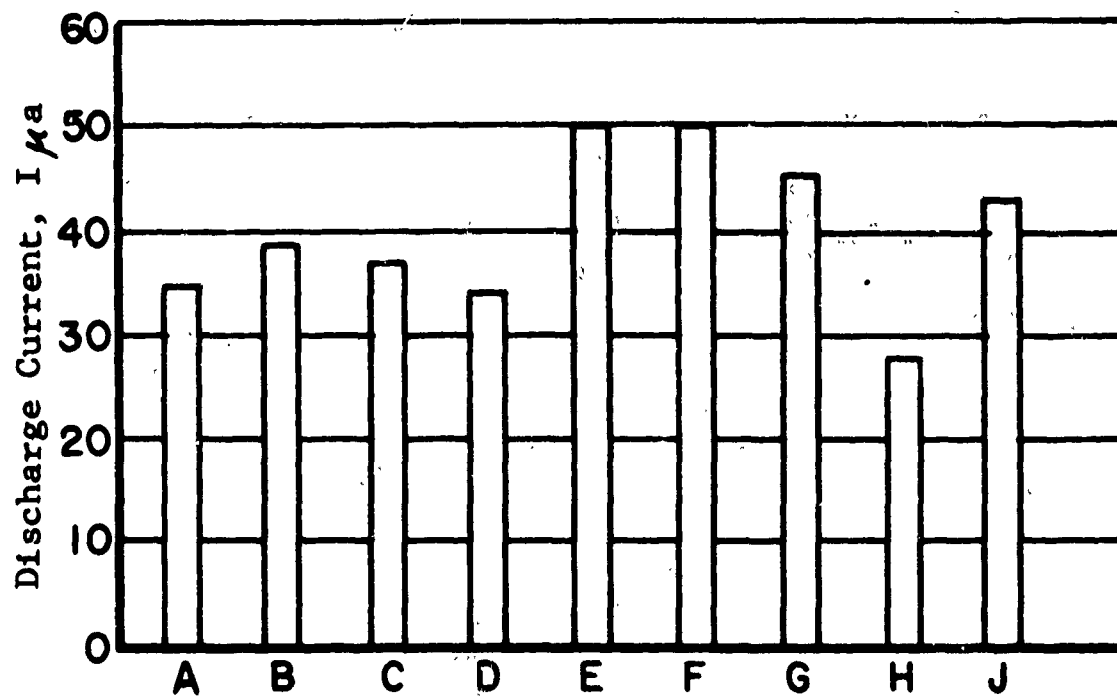
#### CHOOSING CORONA ELECTRODE MATERIAL FOR SECONDARY EMISSION CAPABILITY

The role of secondary emission phenomena in the generation of corona current is represented by the parameter,  $\gamma$ , discussed in Section C, page 13. As stated there, the effect of secondary emission in the physical process of corona discharge does not become significant until the latter stages of the air electrical breakdown. Since electrical breakdown in a corona discharge for a discharging system must be maintained far below the electrical breakdown condition (spark), the use of secondary emission techniques to enhance corona probe performance is not considered practical.

#### CORONA POINT GEOMETRY

As has been previously discussed, corona point geometry and location on the fuselage significantly affect corona point performance. The location of the probe in the maximum downwash velocity region, as suggested in Figure 1, markedly increases corona discharging current. Minimum corona point radius of curvature, as discussed in Section C, also increases corona performance. Practical design aspects, however, limit this radius of curvature within 0.002 to 0.006 inch.

The effect of corona point geometries on discharging current performance has also been investigated in Reference 22. Figure 11, reproduced from Reference 22, compares the performance of several different corona point configurations. As can be seen from this figure, sharp needle probes increase the probe performance. The use of such points, however, is impractical in operational aircraft because of possible injury to ground personnel.



- Probe Type
- A— AN/ASA-3, Wick
  - B— Sharp Needle Probe
  - C— Hollow Cupped Needle Probe
  - D— Solid Cupped Needle Probe
  - E— Radial Cluster Sharp Needle Probe
  - F— Radial Cluster Hollow Needle Probe
  - G— Knife Edge Probe
  - H— 1/4-in-Diameter Cupped Probe
  - J— Thin Wire Probe

Figure 11. Corona Current Discharge for Various Corona Point Configurations (60-Kilovolt Applied Voltage and 90-miles-per-hour Velocity).

## **SECTION G: DISCHARGER SYSTEM OPERATION AND ANALYSIS**

### **THE ELECTROSTATIC DISCHARGER PRINCIPLE**

In the absence of a discharger system, triboelectric or other charging mechanisms will cause the electrostatic charge and, consequently, the potential of the aircraft with respect to its environment to rise steadily. When the resulting electrical field strength in the atmosphere adjacent to the aircraft reaches a critical value of approximately 30 kilovolts per centimeter, natural corona current from random points of the aircraft surface occurs. This corona current is the flow of charge generated by ionization of the atmosphere which occurs when the electrical field becomes sufficiently large, that is, reaches the critical value (see Section C). The rise of aircraft potential is halted only when this flow of charge off the airframe equals the incoming natural charging current. The value of aircraft potential at which corona occurs is determined by the sharpness, that is, radius of curvature of the points on the aircraft surface and therefore varies with the aircraft. A 5-kilovolt potential is a typical threshold voltage causing corona discharge from points of 0.06-inch radius of curvature. The stray discharge current increases as the triboelectric aircraft voltage moves further away from zero until the total corona discharge current equals the charging current, that is, until the net charging current is zero. The amount of charge on the aircraft becomes constant at this time. There is a simple relationship between the charge on the aircraft and its potential provided that the earth is considered the only other conductor present in addition to the aircraft. When this quite valid approximation is made

$$V_H = \frac{Q_H}{C_H} \quad (G-1)$$

where  $V_H$  = aircraft potential relative to earth,

$Q_H$  = aircraft charge, and

$C_H$  = aircraft capacitance.

The value of  $C_H$  varies inversely with the altitude and directly with the area of the aircraft and is, therefore, not constant during flight. Techniques for measuring  $C_H$  are given in Reference 5. The problem arising from aircraft electrostatic charging is due to the magnitude of the residual charge remaining on the aircraft after discharge by natural process.

The dynamic discharger system described in this report prevents excessive rise of potential by automatically controlling the magnitude of corona discharge current from one deliberate corona discharge point on the aircraft. Figure 12 illustrates the system and the charge-discharge current loop. The design and construction of this discharger electrode gives it a superior corona discharge capability. Consequently, the system rapidly brings the net charge current to zero with small residual aircraft charge and potential. Corona occurs only at the discharger probe because the discharger system maintains the aircraft at a potential substantially lower than the corona threshold. The control of discharge current is accomplished by setting the discharge electrode at a potential difference with respect to the aircraft surface by means of a variable voltage generator. This voltage difference determines the field strength about the electrode and, hence, the discharge current as explained in Section D. In effect, the discharger system ionizes the atmosphere at the corona electrode creating a conductive leak-off path at this point for the charge accumulated on the aircraft. The ions of the corona discharge current satisfy the closed-path law of electric current by eventually returning to the particles (dust, snow, et cetera) from which they were triboelectrically removed (see Figure 12). Since natural charging currents of both polarities are possible, the system must be capable of supplying both positive and negative voltage to the corona discharge electrode. The polarity of voltage applied to the corona electrode is that of the electrostatic charge acquired by the aircraft. Thus, both positive and negative corona characteristics are pertinent to the discharger operation.

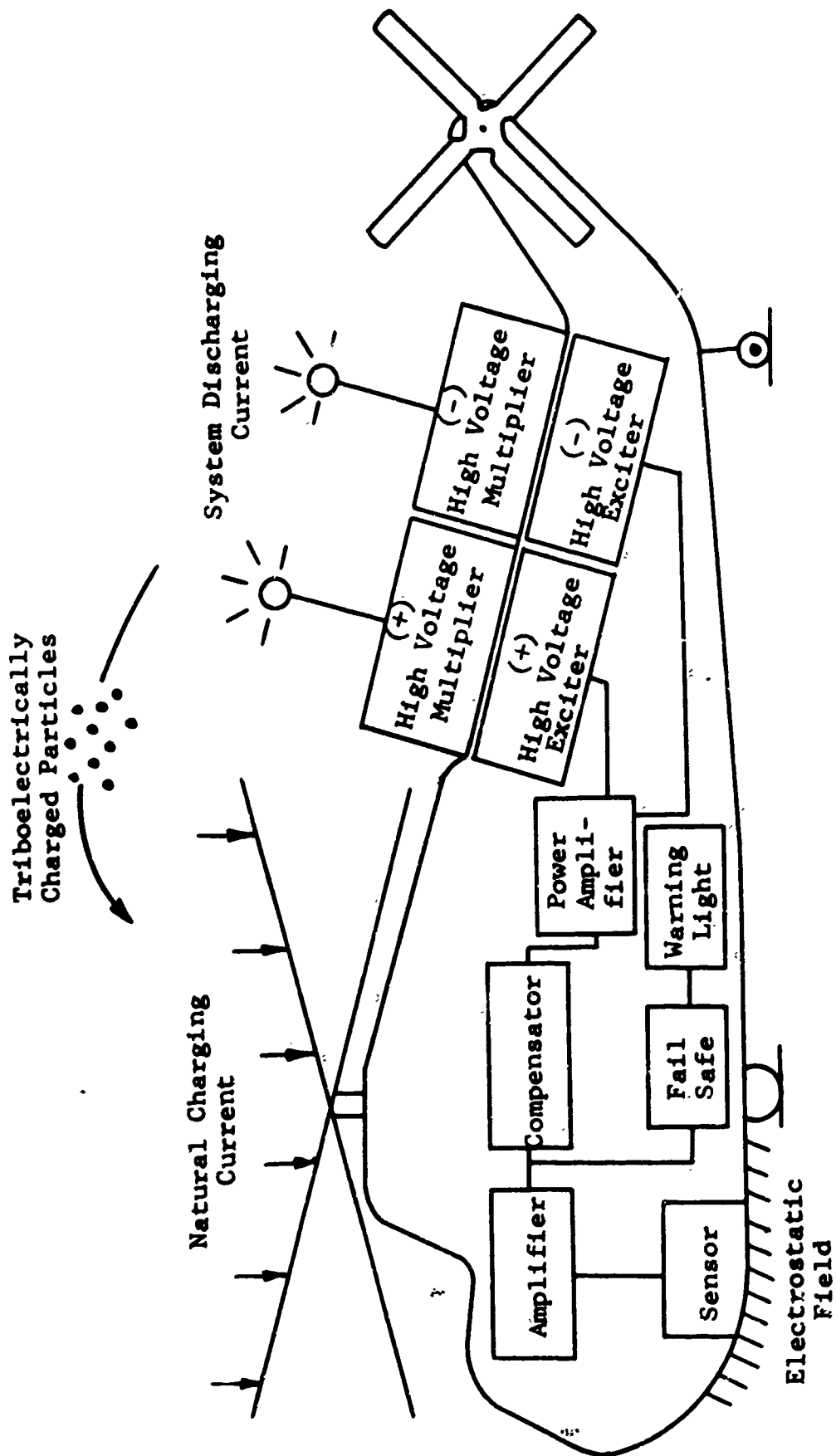


Figure 12. Block Diagram, Aircraft Static Electricity Discharging System.

## DISCHARGER SYSTEM OPERATION

A fully effective discharger system has been constructed by Dynasciences Corporation under USAAML Contract DA 44-177-AMC-114(T). It is basically a feedback amplifier using a sensor of the generating voltmeter type (see system diagram, Figure 13). In operation, aircraft charge is acquired at the rate  $I_n$  predominantly by triboelectric effects on the moving rotor blades of the aircraft. This causes the aircraft to assume a potential,  $V_H$ , with respect to its environment. In most cases, the earth's electrostatic field is small enough to consider this environmental potential as equal to ground potential. The acquired charge also causes an electrical field,  $E_H$ , which is a measure of the potential,  $V_H$ , to exist about the aircraft. The generating voltmeter sensor develops an A.C. signal,  $V_S$ , proportional to  $E_H$  (and hence to  $V_H$  as shown on page 85) which is the input to the control unit. This unit essentially establishes the magnitude and polarity of the corona electrode voltage by the magnitude of its output,  $V_c$ , which will increase or decrease with  $I_n$ . The control unit also contains a compensator circuit which imposes the correct transient response. Without the compensator circuit, the transient response would be determined by the relatively large time constant,  $t_g$ , of the high voltage generator. The system would oscillate excessively or "hunt" if not for this corrective circuit. The power amplifier and high voltage generator develop the large D.C. corona electrode voltage (in the kilovolt range) corresponding to  $V_c$  and the charging current,  $I_n$ . This large D.C. potential causes the atmosphere about the discharger probe to ionize and, consequently, the acquired charge leaves the aircraft at this point. The effective charging current, therefore, is  $I_n - I_d = I_t$ . The system automatically increases the corona electrode voltage until  $I_d = I_n$  or  $I_t = 0$ . The aircraft electrostatic charge ceases to rise at the time the net charging current,  $I_t$ , becomes zero since charge is then leaving the aircraft as fast as it is impinging on it. The amount of charge on the aircraft remains constant once  $I_t$  becomes zero. In combination with the aircraft capacitance,  $C_H$ , this residual charge determines the magnitude of aircraft potential,  $V_H$ . Proper system design using the results of the loop analysis on page 78 insures that the final value of aircraft potential corresponds to an energy level below the

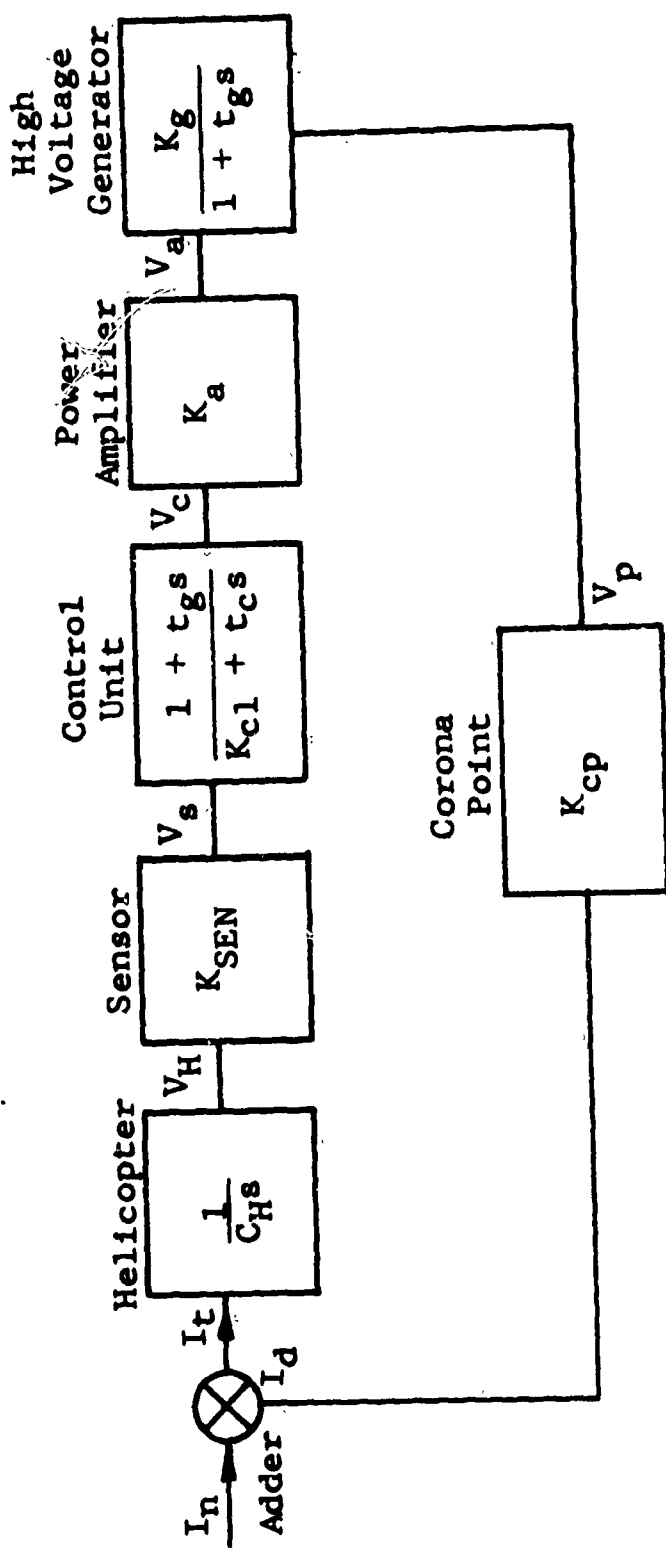


Figure 13. Electrostatic Discharger System Diagram.

danger point (one millijoule) for the given charging conditions. This condition stated mathematically is

$$E_A = \frac{1}{2} C_{HM} V_{HF}^2 = 10^{-3} \text{ joule} \quad (G-2)$$

where  $E_A$  = electrostatic stored energy of aircraft,

$C_{HM}$  = maximum aircraft capacitance (at lowest operating altitude), and

$V_{HF}$  = final aircraft potential.

The value of  $V_{HF}$  is set by the system gain as shown in the loop analysis. The discharger is a servo system because its output,  $I_d$ , affects the magnitude of its effective input,  $I_t$ .

The magnitude of corona discharge increases with the velocity of the airstream sweeping past the corona electrode as discussed in Section D. Consequently, this electrode is positioned under the rotors so that the wind of the rotor downwash improves probe performance as much as possible. Figure 14 on page 76 shows the mounting of the electrode on the fuselage of a tandem rotor helicopter.

The operating effectiveness of the electrostatic discharger system can be checked while in flight at the pilot's cockpit and at the cargo area by means of the failsafe feature. This consists of two control units each having red and green indicator lights. One unit is in the cockpit, the other is at the cargo area. When the discharger system is satisfactorily preventing the rise of aircraft electrostatic charge, the green light is on in both control units. The red light will go on if the sensor is defective, that is, if the sensor voltage output is zero. The red light will also go on if the sensor output is above a specified voltage level. Such an over-voltage indicates an excessive amount of electrostatic charge on the aircraft because of failure of some discharger system unit or extreme operating conditions. When the system is initially energized in charging conditions, the red light will go on. However, when the system has dissipated the excess charge built up before the system was switched on, the green light will normally come on.



**Figure 14. Typical Mounting of Corona Discharge Electrode on a Tandem Rotor Helicopter.**

## LOOP ANALYSIS OF DISCHARGER SYSTEM

The system analyzed here is the generating voltmeter sensor system (GVSS). The purpose of the analysis is to find the time domain system response,  $V_H$ , to a step input,  $I_n$ . To do this, we first find the system parameter,  $V_H/I_n$ , in the s domain and then apply the inverse laplace transform to this parameter to find the time response. The required system parameter is written as the product of two other more easily calculated system parameters. The analysis proceeds as follows, with reference to Figure 13.

$$\frac{V_H}{I_n} = \frac{V_H}{I_o} \cdot \frac{I_o}{I_n} \quad (G-3)$$

The first parameter evaluated is  $I_d/I_n$ . Accordingly,

$$I_t = I_n - I_o \quad (G-4)$$

$$\frac{I_o}{I_n} = \frac{I_o}{I_t + I_o} = \frac{1}{\frac{I_t}{I_o} + 1} = \frac{1}{\frac{I_o}{I_t} + 1} \quad (G-5)$$

The system parameter,  $I_d/I_t$ , appearing in equation (G-5) is the open loop gain,  $F_{OL}$ , given by

$$F_{OL} = \frac{I_o}{I_t} = \frac{K}{C_{NS}(1 + t_{CS})} \quad (G-6)$$

where

$$K = K_{SEN} K_{CS} K_a K_g K_{CP} \quad (G-7)$$

Applying the expression obtained for  $I_d/I_t$  to equation (G-4), one obtains the following result for  $I_d/I_n$ , the closed loop gain:

$$F_{CL} = \frac{I_o}{I_n} = \frac{1}{\frac{C_{NS}(1 + t_{CS})}{K} + 1} \quad (G-8)$$

$$F_{C,I} = \frac{K}{C_H S (1 + t_c s) + K} \quad (G-9)$$

This evaluates one of the two required system parameters. The remaining one is obtained by taking the reciprocal of  $I_d/V_H$ , as follows.

$$\frac{I_d}{V_H} = \frac{K}{1 + t_c s} \quad (G-10)$$

Thus, substituting in equation (G-2)

$$\frac{V_H}{I_n} = \frac{1 + t_c s}{K} \cdot \frac{K}{C_H S (1 + t_c s) + K} \quad (G-11)$$

$$= \frac{1 + t_c s}{K \left( \frac{C_H t_c s^2}{K} + \frac{C_H s}{K} + 1 \right)} \quad (G-12)$$

This is the required network parameter in the s domain.

The laplace transform of the system response to a step input of  $I_n$  is obtained by multiplying  $V_H/I_n$  by the current input transform  $K_x/s$ , where  $K_x$  is the step amplitude. Accordingly, the system response,  $V_H$ , to an input step of  $I_n$  is

$$V_H = \frac{K_x (1 + t_c s)}{K s n \left( \frac{C_H t_c s^2}{K} + \frac{C_H s}{K} + 1 \right)} \quad (G-13)$$

Using Reference 13, the time domain expression for  $V_H/K_x$  derived from this is

$$\frac{V_H}{K_x} = \frac{1}{K} \left[ 1 + \sqrt{\frac{1 - \zeta^2}{1 + \zeta^2}} \sqrt{1 - 2t_c \zeta \omega + t_c^2 \omega^2} e^{-\zeta \omega t} \sin \omega t \right] \quad (G-14)$$

where  $\theta = \left( \omega \sqrt{1 - \zeta^2} \right) t + \psi$

$$\psi = \tan^{-1} \frac{tc\omega^2 \sqrt{1 - \zeta^2}}{1 - tc\zeta\omega} + \tan^{-1} \frac{\sqrt{1 - \zeta^2}}{\zeta}$$

$$\omega = \sqrt{\frac{K}{C_H t_c}}$$

$$\zeta = \frac{1}{2} \sqrt{\frac{C_H}{K t_c}}$$

This is the required result, that is the system response,  $V_H$ , to a step input of charging current,  $I_n$ . From the solution, it is seen that in the steady state, that is when  $t$  becomes infinite

$$\frac{K_x}{V_H} = \dots \quad (G-15)$$

This relationship sets the value of overall system gain,  $K$ , for that electrostatic discharger system which brings the aircraft potential to a specified value for a given charging current.

Also of interest is the value of discharge current,  $I_d$ , in the steady state after a step input of natural charging current,  $I_n$ , has been applied to the system. This is obtained by the use of the expression for closed loop gain,  $F_{c,1}$ , given by equation (G-8). Rewriting this expression

$$F_{c,1} = \frac{I_d}{I_n} = \frac{K}{C_H s (1 + t_c s) + K} \quad (G-16)$$

The laplace transform of  $I_d$  when a step input of  $I_n$  is applied to the system is obtained by multiplying  $I_d/I_n$  by the appropriate current input transform,  $K_x/s$ .  $K_x$  is the step amplitude. Accordingly, the laplace transform of  $I_d$  to such an input is

$$I_o = \frac{KK_x}{s [C_N s (1 + t_c s) + K]} \quad (G-17)$$

The time domain expression for  $I_d$  derived from equation (G-16) is given by Reference 13 as

$$I_d = K_x \left[ 1 + \frac{1}{\sqrt{1 - \zeta^2}} e^{-\frac{t}{2t_c}} \sin(\omega \sqrt{1 - \zeta^2} t - \psi) \right] \quad (G-18)$$

where

$$\omega = \sqrt{\frac{K}{C_N t_c}}$$

$$\zeta = \frac{1}{2} \sqrt{\frac{C_N}{t_c K}}$$

$$\Psi = \tan^{-1} \frac{\sqrt{1 - \zeta^2}}{-\zeta}$$

The fact that  $I_d$  becomes equal to the magnitude of charging current,  $K_x$ , in the steady state, that is when  $t = \infty$  verifies the effectiveness of the system as an electrostatic discharger.

An analog computer analysis of the discharger system dynamics is contained in Appendix II.

#### DESIGN CURVES FOR ELECTROSTATIC DISCHARGER SYSTEM

The quantities necessary to completely specify a discharger system design are:

1. System steady state gain,  $K$ , that is, ratio of charging current to steady state aircraft potential introduced on page 77.

2. Compensator components.
3. Maximum corona electrode voltage which system can apply.
4. Number of corona electrodes required.

The magnitude of these quantities in any particular discharger design is set by the existing values for the following operating conditions:

1. Maximum charging current.
2. Maximum aircraft potential without corona.
3. Aircraft capacitance at operating altitude.
4. Aircraft speed.
5. Time constant of high voltage supply.
6. Required damping ratio.

Curves enabling quick determination of the system specifications for given charging conditions are given in Figure 15. The curves give the required steady state gain, K, compensator components, R<sub>1</sub>, R<sub>2</sub>, and C<sub>C</sub>, and corona electrode voltage, V<sub>p</sub>, over a range of charging conditions for specified damping ratio (0.35) and aircraft electrostatic energy (one millijoule). The curves are entered with the following quantities: natural charging current; I<sub>n</sub>, wind speed; W, helicopter capacitance; C<sub>H</sub>, and high voltage generator time constant; t<sub>g</sub>. Appendix I shows how the data for the curves are calculated. The units to be used with the curves are:

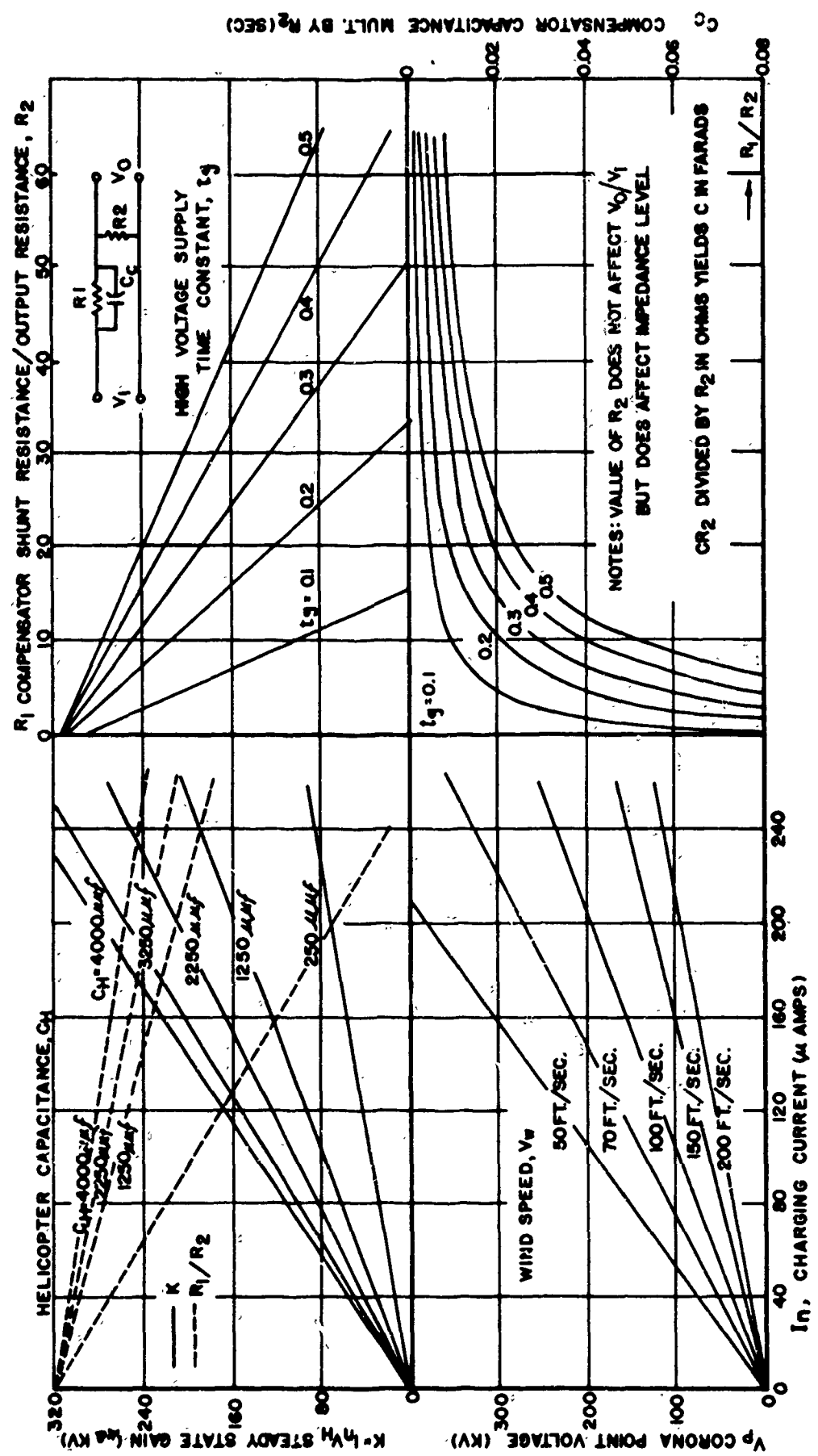
I<sub>n</sub> - microamps

C<sub>H</sub> - micromicrofarads

K - microamps per kilovolt

W - feet per second

V<sub>p</sub> - kilovolts



$t_g$  - seconds

$t_c$  - seconds

R2 - arbitrary

The curves are used as follows.

1. Enter with  $I_n$ .
2. Read  $V_p$  using appropriate wind speed curve.
3. Read K using appropriate solid helicopter capacitance curve in upper left corner.
4. To determine  $R_1/R_2$ , use appropriate dashed helicopter capacitance curve (evaluates  $I_n/C_H$ ) in upper left corner. Then proceed to the appropriate  $t_g$  curve in the upper right corner. Read  $R_1/R_2$  at the intersection of the vertical at this point with the  $R_1/R_2$  axis.
5. To determine  $C_c R_2$ , project the vertical established in step 4 downward to intersect the appropriate  $t_g$  curve in the lower right hand corner. Draw a horizontal at this point of intersection. Read  $C_c R_2$  at the intersection of the horizontal with the  $C_c R_2$  axis.
6. Multiply  $R_1/R_2$  and divide  $C_c R_2$  by the selected value of  $R_2$  to obtain  $R_1$  and  $C_c$ .

#### SENSORS IN ELECTROSTATIC DISCHARGER SYSTEMS

The function of the sensor is to provide electrical information to the discharger system concerning the magnitude of the aircraft potential. The theory and relative merits of three sensors are discussed below. The first of these, the generating voltmeter sensor, has been used in the discharger system because of its superior qualities.

### The Generating Voltmeter Sensor

A rotating vane generating voltmeter produces an A.C. output voltage with an amplitude directly proportional to the field strength of the charged body to which it is attached. When attached to the surface of an electrostatically charged aircraft, this device senses the aircraft potential since, as proven below, the field strength is directly proportional to the aircraft potential. This sensor, however, is ineffective at a point on the aircraft which is in corona. At such a point, charge density no longer builds up as aircraft potential rises; instead, it leaks off into the atmosphere. Hence, the electric field at such points is not proportional to aircraft potential. This type of sensor should therefore be located on the aircraft at a point of minimum curvature. The surface must be convex at the point of location, that is, the curvature must be positive in order for the field strength to be strong enough to cause a sensor response. When located at such a point, the output of this sensor is

$$V_s = K_{SEN} E_H \quad (G-19)$$

where  $E_H$  = field of aircraft surface at sensor location and

$K_{SEN}$  = transfer function of sensor.

It is now shown that if the sensor is placed at a point on the aircraft which is roughly spherical with a radius of curvature of 1 meter, the constant of proportionality,  $K_{SEN}$ , relating the field strength to the aircraft potential has a magnitude very near unity. To see this, consider the potential at such a location on the aircraft surface. Assuming that the surface can here be approximated by an electrically isolated charged sphere,

$$V_H = \frac{q}{4\pi\epsilon_0 R_s} \quad (G-20)$$

where  $q$  = charge on sphere,

$\epsilon_0$  = permittivity of free space, (MKS units),

$R_s$  = radius of curvature, and

$V_H$  = aircraft potential.

Multiplying this ratio by  $R_s/R_s$  gives

$$V_H = \frac{q R_s}{4\pi\epsilon_0 R_s^2} \quad (G-21)$$

According to Reference 8, the electric field at the surface of an aircraft approximated by an isolated sphere of radius,  $R_s$ , is

$$E_H = \frac{q}{4\pi\epsilon_0 R_s^2} \quad (G-22)$$

Therefore, equation (G-20) for  $V_H$  becomes

$$V_H = E_H R_s \quad (G-23)$$

where  $E_H$  = field strength at that point on the aircraft where the curvature is approximately constant with radius,  $R_s$ .

Thus, if  $R_s$  = 1 meter,

$$V_s = K_{SEN} E_H = K_{SEN} \frac{V_H}{R_s} = K_{SEN} V_H \quad (G-24)$$

#### Passive Corona Point Sensor

The system employing this type of sensor is the same as the generating voltmeter sensor system described on page 84 except that the amount of corona current passing through a passive corona point, that is, one connected directly to the aircraft, serves as a sensor of the aircraft potential. The system diagram is that of the GVSS system shown on page 87 except for the sensor transfer function.

In order for the passive corona point to go into corona, the aircraft potential must typically rise to a potential of 3 to 5 kilovolts. Figure 16 is a plot of the transfer function of this type of sensor. Thus, this type of system is incapable of reducing the aircraft potential below 3 to 5 kilovolts. Since this corresponds to an electrostatic energy level above the maximum safe value of one millijoule for most operating conditions (helicopters over 7000-pounds gross weight hovering below twenty-five feet), this system is unacceptable (Reference 4).

### Dynamic Neutralizer Sensor

This device is actually a combination of a potential sensing method and a system concept. A loop analysis appears in Figure 17.

In this system, two high voltage generators are connected with opposite polarity to the aircraft frame at one terminal and to a corona electrode at the other terminal respectively, as shown in Figure 12 on page 72. The voltage output of the generators,  $V_{GPOS}$  and  $V_{GNEG}$ , is adjusted until

$$V_{GPOS} K_{POS} - V_{GNEG} K_{NEG} = 0 \quad (G-25)$$

where  $K_{POS}$  = transfer function of positive corona point, and

$K_{NEG}$  = transfer function of negative corona point.

As described in Section C,  $K_{POS}$  does not equal  $K_{NEG}$  because of differences in the mechanisms of positive and negative corona. To prevent other differences in the corona electrode operating conditions, the relative positions of both corona electrodes with respect to the aircraft and the air speed are made identical. Under these circumstances, and with the aircraft potential zero, the discharge current from both corona electrodes will be equal and the net discharge current will be zero. If the aircraft potential becomes positive (for the acquisition of negative potential all polarities should be reversed in the following discussion) the total potential difference between the positive corona electrode and the surrounding environment increases.

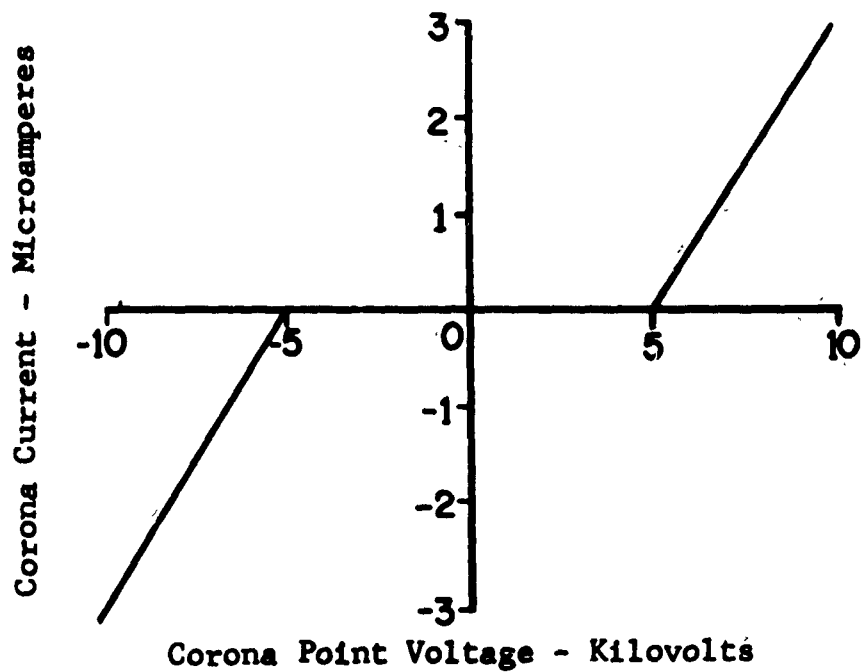


Figure 16. Operation of Passive Corona Point Sensor.

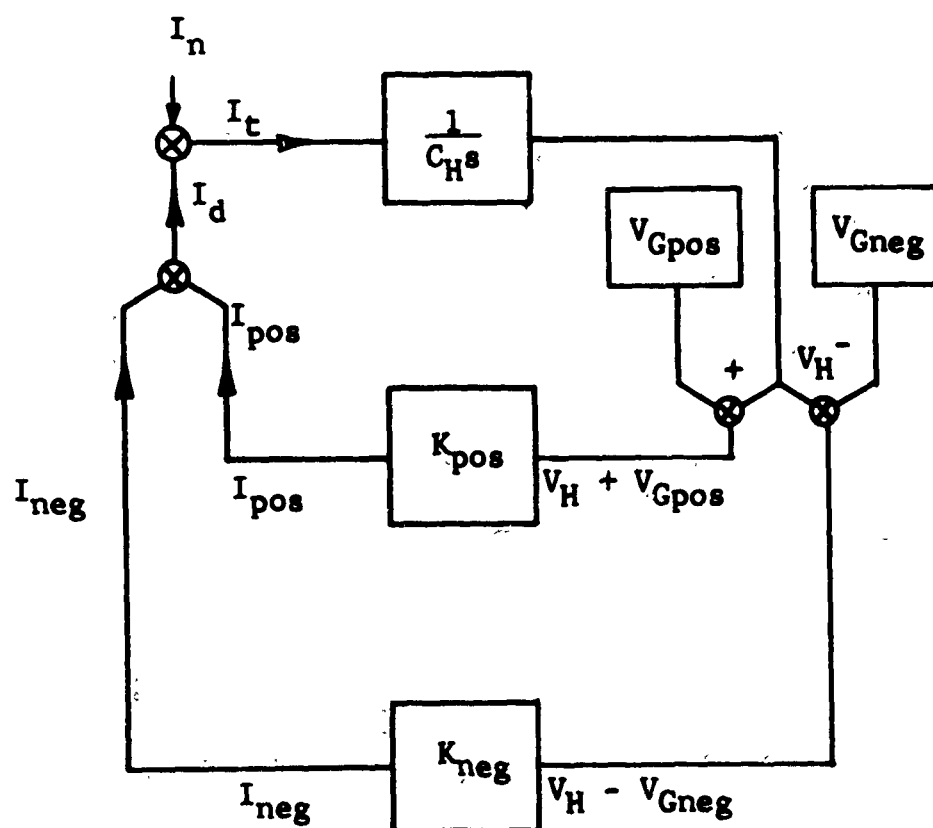


Figure 17. Dynamic Discharger System Diagram.

Also, the total potential difference of the negative corona electrode with respect to its environment decreases. Consequently, the output of the positive corona probe increases and the output of the negative corona probe decreases. As a result of the imbalance of the positive and negative currents, the aircraft takes in a net charge with a polarity that is opposed to that of the natural charge which created the aircraft potential (Reference 4). The system therefore discharges the aircraft.

A loop analysis of the dynamic neutralizer system follows. The mathematical techniques used in the analysis of the GVSS system on page 77 are also used here. The system diagram used is shown in Figure 17.

The purpose of the analysis is to find the time domain response,  $V_H$ , to a step input of  $I_n$  for this system. The required system parameter,  $V_H/I_n$ , is written as the product of two other system parameters. Accordingly,

$$\frac{V_H}{I_n} = \frac{V_H}{I_0} \cdot \frac{I_0}{I_n} \quad (G-26)$$

The first parameter evaluated is  $I_d/I_n$ . We use the following relationship for net charging current.

$$I_t = I_n - I_0 \quad (G-27)$$

Manipulation of equation (G-27) yields

$$\frac{I_0}{I_n} = \frac{1}{\frac{I_t}{I_0} + 1} = \frac{1}{\frac{1}{I_0/I_t} + 1} \quad (G-28)$$

To evaluate  $I_d/I_n$ ,  $I_d/I_t$  is obtained from the analysis which follows.

$$I_0 = I_{POS} + I_{NEG} \quad (G-29)$$

$$= K_{POS}(V_H + V_{GPOS}) + K_{NEG}(V_H - V_{GNEG}) \quad (G-30)$$

$$= V_H(K_{POS} + K_{NEG}) + V_{GPOS}K_{POS} - V_{GNEG}K_{NEG} \quad (G-31)$$

Since  $V_{G\text{pos}} K_{\text{pos}} - V_{G\text{neg}} K_{\text{neg}}$  has been set equal to zero, as described on page 86.

$$I_o = V_H (K_{\text{pos}} + K_{\text{neg}}) \quad (\text{G-32})$$

$$V_H = \frac{I_t}{C_H s} \quad (\text{G-33})$$

$$I_o = \frac{I_t}{C_H s} (K_{\text{pos}} + K_{\text{neg}}) \quad (\text{G-34})$$

and, therefore,

$$\frac{I_o}{I_t} = \frac{K_{\text{pos}} + K_{\text{neg}}}{C_H s} \quad (\text{G-35})$$

Hence, substituting in equation (G-28)

$$\frac{I_o}{I_n} = \frac{\frac{1}{C_H s}}{\frac{K_{\text{pos}} + K_{\text{neg}}}{C_H s} + 1} = \frac{K_{\text{pos}} + K_{\text{neg}}}{C_H s + K_{\text{pos}} + K_{\text{neg}}} \quad (\text{G-36})$$

From equation (G-32)

$$\frac{V_H}{I_o} = \frac{1}{K_{\text{pos}} + K_{\text{neg}}} \quad (\text{G-37})$$

since

$$\frac{V_H}{I_n} = \frac{V_H}{I_o} \cdot \frac{I_o}{I_n} \quad (\text{G-38})$$

Applying equations (G-37) and (G-36) to equation (G-38) gives

$$\frac{V_H}{I_n} = \frac{1}{C_H s + K_{\text{pos}} + K_{\text{neg}}} \quad (\text{G-39})$$

The system response to a step input of  $I_n$  is obtained by multiplying  $V_H/I_n$  by the step input transform,  $K_x/s$ , where  $K_x$  is the step amplitude. Accordingly, the system response,  $V_H$ , to an input step,  $I_n$ , is

$$V_H = \frac{K_X}{C_H s^2 + (K_{POS} + K_{NEG}) s} \quad (G-40)$$

The time domain expression for  $V_H/K$  derived from this is

$$\frac{V_H}{K_X} = \frac{1 - e^{-\left(\frac{K_{POS} + K_{NEG}}{C_H}\right)t}}{K_{POS} + K_{NEG}} \quad (G-41)$$

Equation (G-41) indicates that the dynamic neutralizer is an inherently stable system. However, as has been shown in Reference 4, the gain of this system is insufficient to maintain the helicopter energy within one millijoule at charging rates above 0.5  $\mu$ A.

## CONCLUSIONS

The following conclusions were reached:

1. The theory developed and included in this report predicts discharge system operation consistent with its actual operating characteristics. It therefore puts the discharger system design on a scientific rather than empirical basis.
2. Analytical procedures providing guidelines for discharger system design and optimization have been established by this program.
3. To prevent the loss of discharger system effectiveness caused by return of discharge current to the aircraft, the system discharge electrode should be mounted so that the airstream past the electrode does not strike any part of the aircraft.
4. The amount of polarization in helicopter engine exhaust is too low to improve discharger system performance.

## RECOMMENDATIONS

Several approaches to discharger system performance improvements discussed in Section F of this report should be evaluated experimentally. Specifically, it is recommended that appropriate tests be performed to determine the increase of corona point performance obtainable by the use of radioactive or photoemissive materials.

## BIBLIOGRAPHY

1. Atomic Energy Commission, Title 10, U. S. Government Printing Office, 1963.
2. Born, G.J., Durbin, E.J., An Investigation of Electrical Charging and Discharging of Aircraft in Flight, Report No. 593, Department of Aeronautical Engineering, Princeton University, December 1961.
3. Chapman, S., Discharge of Corona Current from Points on Aircraft or on the Ground, Cornell Aeronautical Laboratory Report No. 66, Buffalo, New York, May 1955.
4. de la Cierva, J., Evaluation of a Helicopter - Fuselage - Mounted Dynamics-Neutralizer Static Electricity Discharging System, TCREC Technical Report 62-93, U. S. Army Transportation Research Command\*, Fort Eustis, Virginia, December 1962.
5. de la Cierva, J., Helicopter Static Electricity Discharging Device, TCREC Technical Report 62-33, U. S. Army Transportation Research Command, Fort Eustis, Virginia, December 1962.
6. Cobine, J.D., Gaseous Conductors, Second Edition, Dover Publications, Inc., New York, New York, 1958.
7. Cornell Aeronautical Laboratory, Study and Evaluation of Methods of Dissipation of Static Electricity on Helicopters, Technical Report 60-55, U. S. Army Transportation Research Command, Fort Eustis, Virginia, September 1960.
8. Frank, N.H., Introduction to Electricity and Optics, Second Edition, McGraw-Hill Book Company, Inc., New York, New York, 1950.
9. Gray, T.S., Applied Electronics, Second Edition, John Wiley and Sons, Inc., New York, New York, 1954.
10. Ingebo, R.D., Drag Coefficients for Droplets and Solid Spheres in Clouds Accelerating in Airstreams, Technical Note 3762, National Advisory Committee for Aeronautics, Washington, D. C., September 1956.

---

\*Changed to U. S. Army Aviation Materiel Laboratories in March 1965.

11. Loeb, L.B., Basic Processes of Gaseous Electronics, Second Edition, University of California Press, Berkeley and Los Angeles, California, 1961.
12. Loeb, L.B., "Recent Developments in Analysis of the Mechanisms of Positive and Negative Coronas in Air", Journal of Applied Physics, Volume 19, October 1948, pp. 883-897.
13. Nixon, F.E., Principles of Automatic Controls, Prentice-Hall, Inc., Englewood Cliffs, New Jersey, 1953.
14. Nanevitz, J.E., Vance, E.F., Tanner, R.L., Hilbers, G.R., Development and Testing of Techniques for Precipitation Static Interference Reduction, ASD-TDR-62-38, Aeronautical Systems Division, Wright-Patterson Air Force Base, Ohio, January 1962.
15. Philco Corporation, Final Engineering Report on Precipitation Static Reduction, U. S. Air Force Contract No. W33-038AC 20763, Philadelphia, Pennsylvania, 9 February 1950.
16. Pierce, E.T., Nadile, R.M., McKinnon, P.J., An Experimental Investigation of Negative Point-Plane Corona and Its Relation to Ball Lightening, AFCLR-TR-60-354, Air Research and Development Command, United States Air Force, Bedford, Massachusetts, 24 October 1960.
17. National Science Foundation, American Institute of Physics Handbook, Second Edition, McGraw-Hill Book Company, Inc., New York, New York, 1963.
18. Tanner, R.L., Radio Interference from Corona Discharges, Stanford Research Institute Project No. 591, California, April 1953.
20. Semat, H., Introduction to Atomic Physics, Rinehart and Company, Inc., New York, New York, 1946.
21. Dynasciences Corporation, A High Performance Electrostatic Discharger for Helicopters, TCREC Technical Report 63-43, U. S. Army Transportation Research Command, Fort Eustis, Virginia, September 1963.

22. de la Cierva, J., et al, Investigation of an Electro-magnetic Interference-Free Active Static Discharging Technique for Fixed and Rotary Wing Aircraft, Air Force Avionics Laboratory Technical Documentary Report No. AL-TDR-64-35, August 1964.
23. Handbook of Chemistry and Physics, Forty-Fourth Edition, The Chemical Rubber Publishing Co., Cleveland, Ohio, Reprint April 1962.

## DISTRIBUTION

US Army Materiel Command	2
US Army Mobility Command	2
US Army Aviation Materiel Command	3
Chief of R&D, D/A	2
US Army Aviation Materiel Laboratories	42
US Army Engineer R&D Laboratories	2
US Army Limited War Laboratory	1
Army Research Office-Durham	1
US Army Combat Developments Command, Fort Belvoir	1
US Army Combat Developments Command Transportation Agency	1
US Army Combat Developments Command Experimentation Command	1
US Army War College	1
US Army Command and General Staff College	1
US Army Transportation School	1
US Army Aviation School	1
US Army Quartermaster School	1
US Army Transportation Center and Fort Eustis	1
US Army Infantry Center	1
US Army Aviation Test Board	1
US Army Arctic Test Center	1
US Army Electronics Command	1
US Army Aviation Test Activity	1
US Army Transportation Engineering Agency	1
Air Force Flight Test Center, Edwards AFB	1
Air Proving Ground Center, Eglin AFB	1
Air Force Avionics Laboratory, Wright-Patterson AFB	1
Chief of Naval Research, D/N	1
US Naval Air Station, Patuxent River	1
Marine Corps Educational Center	1
Marine Corps Liaison Officer, US Army Transportation School	1
Testing and Development Division, US Coast Guard	1
Ames Research Center, NASA	1
Lewis Research Center, NASA	1
Manned Spacecraft Center, NASA	1
NASA Representative, Scientific and Technical Information Facility	2
Research Analysis Corporation	1
NAFEC Library (FAA)	1
Defense Documentation Center	20
US Government Printing Office	1

## APPENDIX I

### DERIVATION OF EQUATIONS FOR DESIGN CURVES

The values of  $K$ ,  $R_1$ ,  $C_C$ , and  $V_p$  required to obtain the curves are found by simultaneously solving the six equations which apply in terms of  $I_n$ ,  $W$ ,  $C_H$ , and  $t_g$ . These equations are

$$E = \frac{1}{2} C_H V_H^2 \quad (\text{APPI-1})$$

$$K = I_n / V_H \quad (\text{APPI-2})$$

$$\zeta = \frac{1}{2} \sqrt{\frac{C_H}{K t_c}} \quad (\text{APPI-3})$$

$$I_n = I_o = K C_P \frac{W}{W_C} V_p \quad (\text{In steady state}) \quad (\text{APPI-4})$$

$$R_1 C_C = t_g \quad (\text{APPI-5})$$

$$\frac{R_1 R_2 C_C}{R_2 + R_1} = t_C \quad (\text{APPI-6})$$

Equation (APPI-4) is a linearization of the discharge current - wind speed dependence at a given  $V_p$ . Equations (APPI-5) and (APPI-6) come from the condition that the compensator transfer function be given by

$$\frac{V_o}{V_i} = K_C I \left[ \frac{1 + t_g s}{1 + t_C s} \right] = \left( \frac{R_2}{R_1 + R_2} \right) \left( \frac{1 + R_1 C_C s}{1 + \frac{R_1 R_2 C_C s}{R_1 + R_2}} \right) \quad (\text{APPI-7})$$

for the compensator circuit as shown on the curves. The constants in the above equations and their values used in constructing the curves are as follows.

$$\mathcal{E} = \text{permissible helicopter electrostatic energy} \quad 10^{-3} \text{ joule}$$

$$\zeta = \text{system damping ratio} \quad 0.35$$

$$K_{CP} \text{ transfer function of corona point (a two-point probe)} \quad 0.835 \mu\text{amp/Kv}$$

$$W_c, \text{ value of wind at which } K_{CP} \text{ was measured} \quad 80 \text{ ft/sec}$$

Solving the equations and applying suitable constants to allow the use of convenient units yields

$$K = 0.0224 I_n \sqrt{C_H} \quad (\text{APPI-8})$$

$$V_p = 96.0 I_n W \quad (\text{APPI-9})$$

$$\frac{R_1}{R_2} = 11.0 t_g \frac{I_n}{\sqrt{C_H}} - 1.0 \quad (\text{APPI-10})$$

$$C_c R_2 = \frac{t_g}{R_1/R_2} \quad (\text{APPI-11})$$

## APPENDIX II

### ANALOG COMPUTER ANALYSIS OF DISCHARGER SYSTEM DYNAMICS

An analog computer analysis of the discharger system dynamics was performed. The system equations are as follows.

$$I_t = I_n - I_d$$

(APPII-1)

$$V_n = \frac{I_t}{C_n s}$$

(APPII-2)

$$V_s = K_{sn} V_n$$

(APPII-3)

$$V_c = K_{ci} V_s$$

(APPII-4)

$$V_a = K_a V_c$$

(APPII-5)

$$V_p = \frac{K_g}{1 + tgs} V_a$$

(APPII-6)

$$I_d = K_{dp} V_p$$

(APPII-7)

The symbols are defined in the block diagram shown in Figure 18 of this appendix. Values for the system constants are as follows.

$$C_n = 10^{-7} \text{ FARADS}$$

(APPII-8)

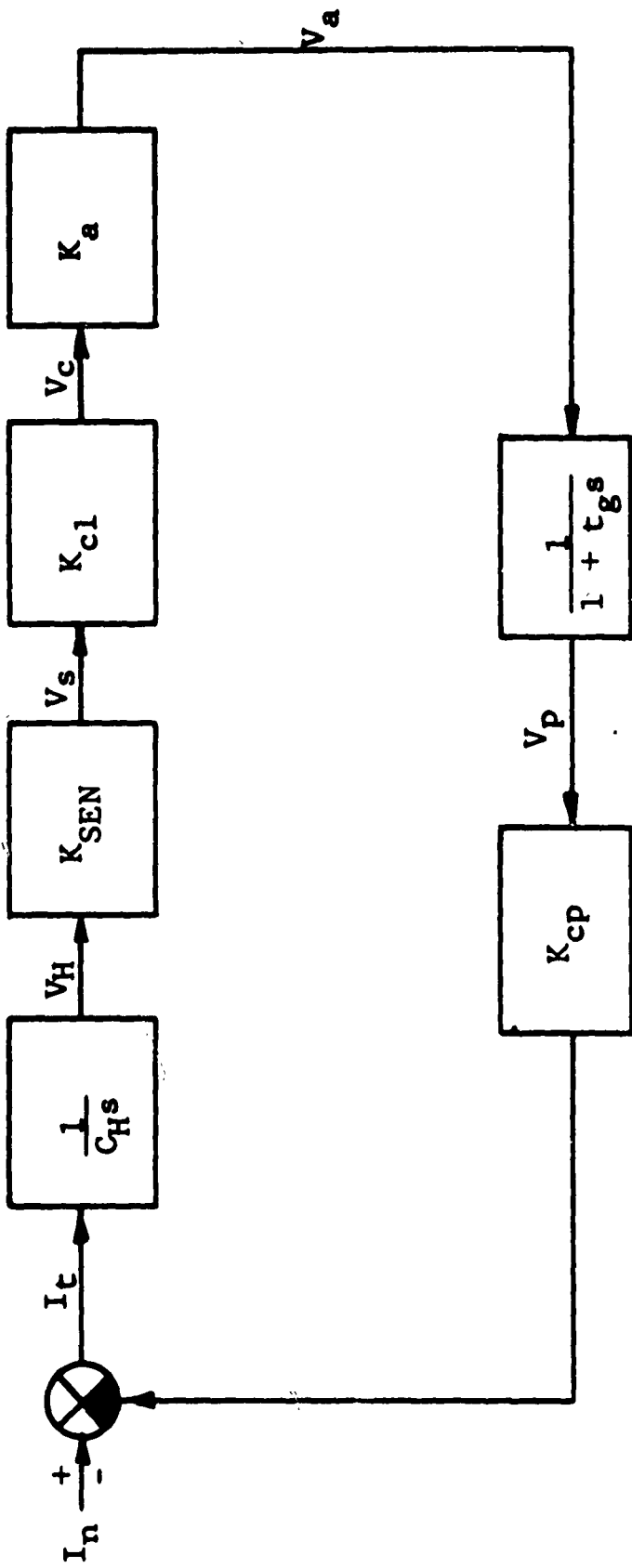


Figure 18. GVSS Electrostatic Discharger Functional Block Diagram.

$$C_H = 10^{-9} \text{ farads} \quad (\text{APPII-8})$$

$$K_{\text{SEN}} = 3 \times 10^{-3} \frac{\text{VOLTS PEAK}}{\text{VOLTS D.C.}} \quad (\text{APPII-9})$$

$$K_{c1} = \text{to be varied between } 2.67 \times 10^{-3} \text{ and } 13.31 \times 10^{-3} \frac{\text{VOLTS PEAK}}{\text{VOLTS PEAK}} \quad (\text{APPII-10})$$

$$K_a = 10^3 \frac{\text{VOLTS PEAK}}{\text{VOLTS PEAK}} \quad (\text{APPII-11})$$

$$K_g = 2.5 \times 10^3 \frac{\text{VOLTS DC}}{\text{VOLTS PEAK}} \quad (\text{APPII-12})$$

$$t_g = \text{to be varied between } 0.03 \text{ and } 0.5 \text{ second} \quad (\text{APPII-13})$$

$$K_{cp} = 0.835 \times 10^{-9} \frac{\text{AMPERES DC}}{\text{VOLTS DC}} \quad (\text{APPII-14})$$

The machine equations used in the computer are

$$\frac{I_t}{5 \times 10^{-5}} = \frac{I_n}{5 \times 10^{-5}} - \frac{I_d}{5 \times 10^{-5}} \quad (\text{APPII-15})$$

$$\frac{V_H}{2000} = \frac{25}{S} \left[ \frac{I_t}{5 \times 10^{-5}} \right] \quad (\text{APPII-16})$$

$$\frac{V_S}{10} = 0.6 \left[ \frac{V_H}{2000} \right] \quad (\text{APPII-17})$$

$$\frac{V_c}{0.05} = 0.2 \left[ 10^3 K_{c1} \right] \left[ \frac{V_S}{10} \right] \quad (\text{APPII-18})$$

$$\frac{V_a}{50} = \frac{V_c}{0.05} \quad (\text{APPII-19})$$

$$\frac{V_p}{6 \times 10^4} = \frac{2.09}{1 + t_g s} \left[ \frac{V_a}{50} \right] \quad (\text{APPII-20})$$

$$\frac{I_d}{5 \times 10^{-5}} = \frac{V_p}{6 \times 10^4} \quad (\text{APPII-21})$$

The analog computer diagram of equations (APPII-15) through (APPII-21) is presented in Figure 19 of this appendix. The helicopter voltage response ( $V_H/2000$ ) was obtained to step inputs of the natural charging current ( $I_n/5 \times 10^{-5}$ ).

As expected, the system stability increased with a decrease of  $t_g$ . A value of  $t_g < 0.1$  second provides good system stability.

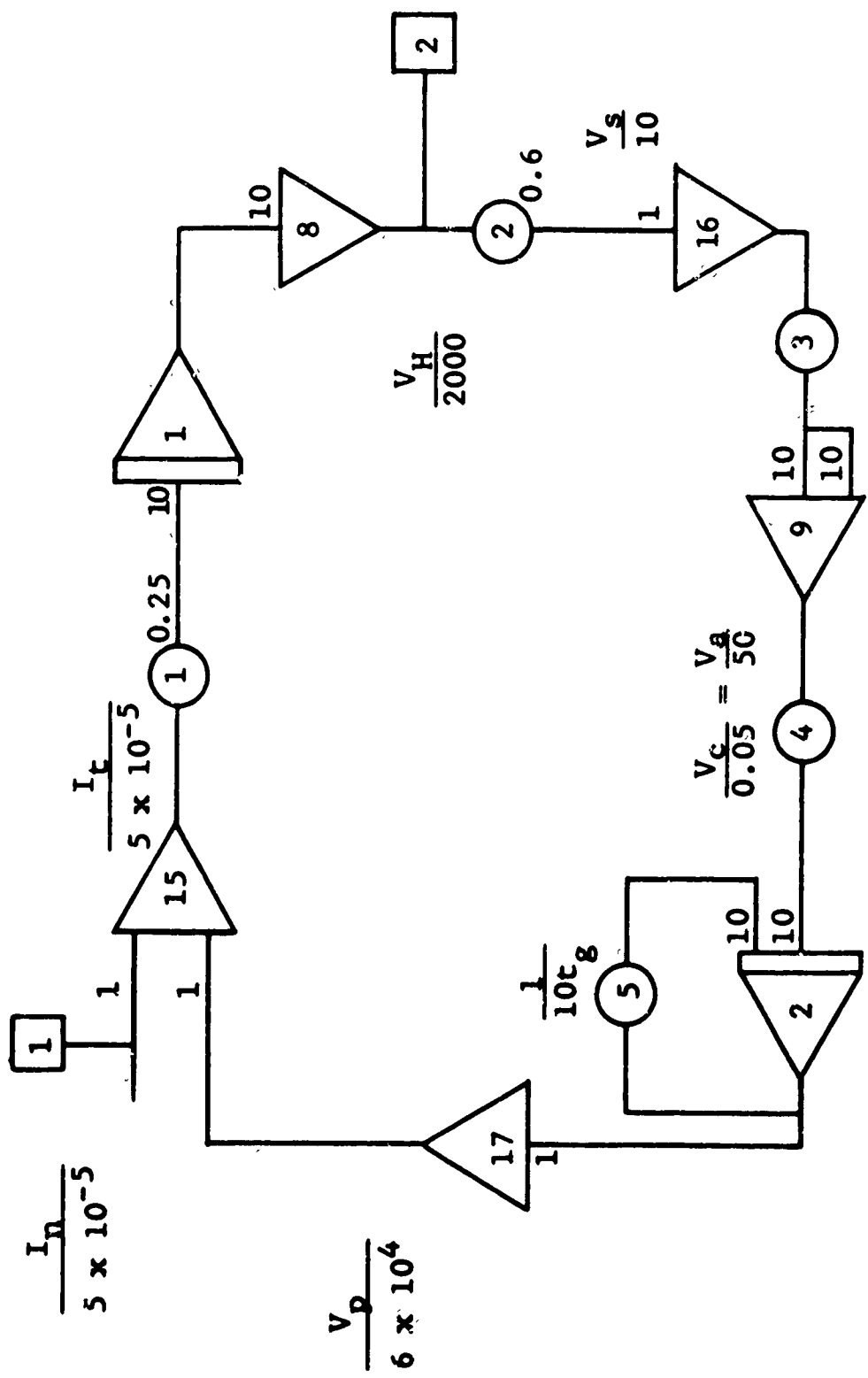


Figure 19. Analog Computer Diagram.